Environmental and Experimental Botany 218 (2024) 105586

Contents lists available at ScienceDirect

Environmental and Experimental Botany

journal homepage: www.elsevier.com/locate/envexpbot

Response to salinity stress in four *Olea europaea* L. genotypes: A multidisciplinary approach

Emily Rose Palm [a,b], Anna Maria Salzano [c], Marzia Vergine [d], Carmine Negro [d], Werther Guidi Nissim [a,b,j,*], Leonardo Sabbatini [a], Raffaella Balestrini [e], Maria Concetta de Pinto [f], Stefania Fortunato [f], Gholamreza Gohari [g,h], Stefano Mancuso [a,i], Andrea Luvisi [d], Luigi De Bellis [d], Andrea Scaloni [c], Federico Vita [a,f]

[a] *Department of Agriculture, Food, Environment and Forestry, University of Florence, Florence 50121, Italy*
[b] *Department of Biotechnology and Biosciences, University of Milano-Bicocca, Milano 20126, Italy*
[c] *Proteomics, Metabolomics and Mass Spectrometry Laboratory, Institute for the Animal Production System in the Mediterranean Environment, National Research Council, Portici 80055, Italy*
[d] *Department of Biological and Environmental Sciences and Technologies, University of Salento, Lecce 73100, Italy*
[e] *Institute for Sustainable Plant Protection, National Research Council of Italy, Torino 10135, Italy*
[f] *Department of Biology, University of Bari "Aldo Moro", Bari 70121, Italy*
[g] *Department of Horticultural Science, Faculty of Agriculture, University of Maragheh, Maragheh 97HF+498, Iran*
[h] *Department of Agricultural Sciences, Biotechnology and Food Science, Cyprus University of Technology, Limassol 3036, Cyprus*
[i] *Fondazione per il futuro delle città (FFC), Florence 50121, Italy*
[j] *NBFC, National Biodiversity Future Center, Palermo 90133, Italy*

ARTICLE INFO

Keywords:
Olive tree
Plant biodiversity
Plant physiology
Proteomics
Response to salt stress
Salinity

ABSTRACT

Despite a drought- and erosion-tolerant root system, olive trees are vulnerable to abiotic stress due to limited genetic variability. Though some olive cultivars are moderately tolerant to salinity stress, soil salinity is increasing in the semi-arid and arid regions where olive cultivation is common, significantly reducing overall production. In response, breeding programs may rely on proper selection markers for abiotic stresses, including salinity, but these are generally lacking for olive. Here, physiological and biochemical parameters were measured in four *Olea europaea* genotypes (Frantoio, Leccino, Lecciana, and Oliana) subjected to different intensities of salinity stress (0 mM, 100 mM and 200 mM NaCl). At moderate and high salt concentrations, Na^+ exclusion, higher photosynthetic productivity and tissue water content in the tolerant cultivar Frantoio were linked with increased production of polyphenols, with more favorable K^+/Na^+ values (quercetin and rutin), mitigation of oxidative stress (oleuropein) and increased water absorption (luteolin). In Frantoio and Leccino, a significant change of the proteome repertoire occurred, with overrepresentation of components regulating cellular metabolism, ion transport, redox insult and dissipation of excess photochemical energy. Conversely, Lecciana and Oliana showed increased sensitivity to salinity stress in terms of photosynthetic parameters and elevated internal Na^+ concentrations, together with the lowest number of differentially represented proteins. These results highlighted olive germplasm strategies to cope with osmotic stress, suggested a physiological and molecular basis for the augmented responsiveness of tolerant cultivars and identified specific biomarkers as useful targets for future breeding programs.

1. Introduction

Globally salinization is a major threat for crop production. 3% of the Earth's surface is currently considered occupied by salt-affected soils, mainly occurring in the arid and semiarid regions of Asia, Australia, and South America (Tóth et al., 2008). In Europe, saline soils are mostly present in the Caspian Basin, Ukraine, the Carpathian Basin, the Iberian Peninsula (Tóth et al., 2008), and southern Europe (Daliakopoulos et al., 2016). In the Mediterranean region, increases in soil salinity could directly impact the production of olive, a valuable crop of historical

* Correspondence to: Department of Biotechnology and Biosciences, University of Milano-Bicocca, Piazza della Scienza 2, Milano 20126, Italy.
E-mail address: werther.guidinissim@unimib.it (W. Guidi Nissim).

https://doi.org/10.1016/j.envexpbot.2023.105586
Received 22 September 2023; Received in revised form 23 November 2023; Accepted 28 November 2023
Available online 1 December 2023

significance that has dominated the local economy and the rural landscape for over six million years (Besnard et al., 2018). The demand for and consumption of olive oil are consistently increasing (El Otmani et al., 2021); for this reason, new olive tree orchards have been developed in all parts of the world, many of which focus on super high-density (SHD) olive crop systems (Tous, 2011). However, few traditional olive cultivars meet the low vigor required by SHD systems, and increasing soil salinity puts further stress on dwindling land resources. To meet the growing demand, cultivars should be tolerant to both SHD cultivation and soil salinity.

The main symptoms of salinity stress in plants are chlorosis and necrosis of leaves, desiccation of flowers and new shoots, and leaf abscission after a long period of stress (Carillo et al., 2011). Olive trees grown in saline soils show reductions in growth, thickened mesophyll tissues and cell walls, reduced blooming, decreased pollen germinability, and fewer fruits (Gucci et al., 1997). Leaf drop of the oldest leaves may be the last defense mechanism against high salt concentrations, simultaneously reducing levels of toxic ions (Na^+ and Cl^-) and the transpiration rate of the whole plant, as salt accumulation progresses from bottom to top (Loupassaki et al., 2002). Plants may counteract or avoid salinity stress with different strategies: i) tolerance to osmotic stress, resulting in increased leaf area, ii) Na^+ exclusion from roots and leaf blades, and iii) tissue tolerance to accumulated Na^+ or Cl^- levels (Munns and Tester, 2008). Woody plants share similar mechanisms for facing salinity stress with non-woody plants (Llanes et al., 2021). However, due to the cost and time required to obtain fruit yields because of a long juvenile phase, woody crop tolerance to salinity stress has mainly been determined only for the vegetative growth phase (Maas and Grattan, 2015). The additional detrimental effects caused by specific ion toxicities have led to the conclusion that most fruit tree and nut crops are salinity-sensitive. In contrast, olive and a few other species are thought to be moderately salinity-tolerant species (Gucci and Tattini, 2010; Maas and Grattan, 2015).

Several studies have shown that the olive tree's ability to cope with high salt concentrations is closely related to efficient ion exclusion and retention by the roots (Chartzoulakis et al., 2002). Advances have been made in the molecular characterization of salinity stress responses through different *omics* approaches (Mousavi et al., 2019, 2022), including proteomics (Skodra et al., 2023). An original study on olive response to salinity stress demonstrated a 30–50% enhancement in protein content and activity of the main NADPH-recycling enzymes, such as glucose-6-phosphate dehydrogenase and ferredoxin-NADP reductase (Valderrama et al., 2007). This dramatic increase indicates that olive induces several antioxidant enzymes to cope with oxidative damage. Proteomic changes in the 'Chétoui' olive cultivar were observed when irrigation water containing 200 mM NaCl was used (Ben Abdallah et al., 2018), including osmotic stress-driven downregulation of proteins involved in photosynthetic processes, bark storage components, glutamine synthetase cytosolic isozymes, salicylic acid-binding protein, and carbonic anhydrase. Despite these pioneering studies, research on the response of olive trees to salinity stress lacks a detailed assessment through the newest high-throughput technologies, such as the gel-free proteomic approaches based on tandem mass tagging (TMT) for relative protein quantitation.

The current study aimed to investigate salinity tolerance in olive tree by identifying reliable descriptors capable of discriminating between four cultivars having a varying response to salinity stress conditions. This result was achieved using a multidisciplinary approach based on phenotypic and physiological analyses (i.e., gas exchange, water content, and ion relations) to investigate the effect of different substrate and salinity levels on the physiology of olive cultivars. In parallel, a complete proteomic picture of the plant response to salinity stress in olive cultivars was obtained through a TMT-based approach. Finally, the ability to produce secondary metabolites in response to salinity was tested through a dedicated metabolomic analysis.

2. Materials and methods

2.1. Experimental setup

The present study was performed on two-year-old self rooted cuttings of four olive genotypes, Frantoio (FR), Leccino (LE), Lecciana (LA) and Oliana (OL), which were exposed to control and two salinity stress conditions (0 mM, 100 mM and 200 mM NaCl) according to the experimental scheme summarized in Fig. S1. LA and OL were purchased from Agromillora (https://www.agromillora.com/it/), whereas FR and LE from Vivai Pietro Pacini (Pescia, Italy). LA and OL are generally considered adapted for super-high density (SHD) cropping systems. Conversely, FR and LE are Italian cultivars having a constant yield with high and medium vigor, respectively, which limits their use in SHD systems. FR has been previously described as being more tolerant to salinity stress than LE (Tattini, Melgar and Traversi, 2008; Cimato et al., 2010). Forty-five plants of each cultivar were transplanted into polyethylene pots (8×8x18cm) containing approximately 1.15 dm^3 of sterilized perlite substrate (Agrilit 3, Agriperlite Italiana, Alzaia Trento, Italy). Plants were grown in a greenhouse at the University of Florence (Italy) (lat. 43°48′58.6″ N, long. 11°11′58.1″ E) from June to September 2019 with semi-controlled conditions: natural, non-supplemented lighting (average 500 μmol m^{-2} s^{-1} PAR), mean air temperature 28 °C (T_{Max} 34.5 °C –- T_{min} 24.9 °C), mean air humidity 46% (max 60.5% - min 34.4%) and a photoperiod of 15 h light/9 h dark. Plants were watered through a circulating bench subirrigation system, which filled the benches until half of the height of the pots (4 cm) was reached in 5 min with an outflow after 15 min. Following the acclimation period of one month after transplanting, different NaCl concentrations were applied: 0 mM (control), 100 mM and 200 mM NaCl, using a half-strength Hoagland solution (Hoagland and Arnon, 1938) for nutrient supply. A total of 15 plants (n = 15) were used for each treatment within each of the four cultivars. To avoid osmotic shock, NaCl concentration values were increased gradually by adding 50 mM NaCl every two days until the final concentration values were reached (Ben Abdallah et al., 2018). EC and pH of the solution reservoirs were checked weekly with a portable conductivity meter and adjusted if necessary with HNO_3, and water added until to a final volume of 300 L. The set values for EC/pH were 1542.08 μS cm^{-1}/6.8 for 0 mM NaCl (control), 10.44 mS cm^{-1} /6.8 for 100 mM NaCl, and 19.07 mS cm^{-1} /6.8 for 200 mM NaCl.

2.2. Biometric determination and physiological analyses

At the end of the trial, ten plants per treatment were separated into leaves, stems, and roots and fresh weight (FW) was determined. Roots were washed to remove residual perlite, and tissues dried at 70 °C until constant weight to determine dry weight (DW). Gas exchange measurements were performed on the first fully expanded leaf from the top of each cultivar using a portable LI-COR 6400XT instrument (LI-COR Inc., Lincoln, NE, USA) on five plants per cultivar, every week, for eight weeks between 08:00 and 13:00. Net carbon assimilation rate (A_n), stomatal conductance (g_s), and intercellular CO_2 concentration (C_i) were performed with the following settings: CO_2 concentration: 400 μmol CO_2 mol^{-1}; block temperature: 28 °C; PAR: 1000 μmol m^{-2} s^{-1}; relative humidity: 50–60%. Dark-adapted (Fv/Fm) and light-adapted (Fv'/Fm') maximum and effective quantum yield, respectively, of PSII and non-photochemical quenching (NPQ) were measured on three replicates for each experimental condition. For the light-adapted leaves, a light intensity of 1000 μmol m^{-2} s^{-1} PAR was used, and Fv'/Fm' and NPQ values were taken 5 min after the light was switched on to ensure the transition of leaves to the light adapted state.

2.3. Analysis of Na^+ and K^+ content in the biomass

Subsamples from the dried stem, leaf and root biomass of 6 plants from each treatment for each cultivar were ground with a hammer mill.

0.5 g of oven-dried ground biomass was mineralized following the Aqua Regia extraction method using a Mars6 Xpress microwave system (CEM® Matthews, NC, USA) following the protocol described in Guidi Nissim et al. (2021). Digested samples were diluted to a final volume of 50 mL with Milli-Q water and then analyzed using a Flame Photometer Digiflame2000 DV 704 (Lab Services SAS, Rome, Italy). A calibration curve with values ranging from 0 to 0.1 mg mL^{-1} for Na^+ and K^+ ($R^2 = 0.998$) was used for ion content determination. A certified reference material of ryegrass (ERM® – CD281 RYE GRASS, European Commission, Joint Research Centre, Institute for Reference Materials and Measurements, Belgium) was digested alongside the samples with method blanks and duplicate samples for method validation.

2.4. Metabolomic analysis

The effect of salinity stress on the polyphenolic profiles of all four cultivars was assessed through a metabolomic analysis of leaves collected after eight weeks. Twenty leaves from three plants per cultivar and treatment combination were collected from the middle of the main axis and ground with a pestle and mortar in liquid nitrogen. 0.5 g of ground leaves were weighed in a 15 mL bag (BIOREBA, Reinach, Switzerland) and 5 mL of extraction buffer (methanol/water/formic acid, 60:39.9:0.1 v/v/v), pH 2.8 (Fisherbrand ™ accumet ™ AB200 coupled with cat. 1726358 sleeve junction pH electrode) was added and centrifuged at 5000 g, at 23 °C, for 10 min. The supernatant was filtered into glass vials using a 0.2 μm polytetrafluoroethylene membrane. Three replicates for each harvested sample were carried out. Leaf extracts were then subjected to HPLC ESI/MS-TOF analysis for quali-quantitative determination of corresponding polyphenols using appropriate standards (Fig. 5), and then without standards (Table S5) as a method to identify a wider range of compounds. Retention times, experimental and calculated *m/z* values, and molecular formulas of phenolic compounds identified through chemical standards are reported in Table 1. Metabolite characterization and quantification were performed using an Agilent 1200 liquid chromatography system (Agilent Technologies, Palo Alto, CA, USA) equipped with a standard autosampler and analytical column Agilent Zorbax extended C18 (5 × 2.1 cm, 1.8 μm) as previously described (Vergine et al., 2022). For external standard calibration, the following compounds were used: quinic acid, quercitrin, hydroxytyrosol glucoside, luteolin, luteolin 7-O glucoside, oleuropein glucoside, rutin, and verbascoside. Data elaboration was carried out using the Mass Hunter software (Agilent Technologies). The limit of quantification (LOQ) was determined as the signal-to-noise ratio of 10.1, and the limit of detection (LOD) was established as a 3:1 ratio.

2.5. Proteomic and bioinformatic analyses

Leaf tissue samples (100 mg) from three plants per treatment group were ground to a fine powder, and protein extraction was obtained through homogenization in 10% w/v TCA, 0.07% v/v ß-mercaptoethanol in cold acetone, as detailed in Supporting Information. Protein samples for relative quantification were processed using a modified FASP method (Wiśniewski et al., 2009), labeled with TMT mass tagging kit (Thermo-Fisher Scientific) and then analyzed by nanoLC-ESI-MS/MS with a Q-ExactivePlus mass spectrometer (Thermo-Fisher Scientific), as detailed in Supporting Information. Mass spectrometry raw data were analyzed for protein identification and relative quantification by Proteome Discoverer (Thermo) using Mascot (Matrix Science) against a home-made databases of protein sequences. The results were filtered to include only significant data showing an abundance ratio < 0.5 or > 2.0 with p-value < 0.05, that were considered as differentially represented proteins (DRPs). Statistical and functional analysis was performed as previously reported (Salzano et al., 2019). All experimental and technical details have been reported in Supporting Information.

2.6. Statistical analysis

The data from biometric, photosynthetic, ion and polyphenolic analyses were assessed for normal distribution through a Shapiro Wilk test, and then analyzed using two-way ANOVA analyses followed by Tukey's honestly significant difference (Tukey's-HSD) post hoc test ($p \leq 0.05$) within each cultivar. Data from polyphenolic determinations were also analyzed using PCA, and results were graphically processed to highlight the contribution of each variable (compounds) and the differentiation of the observations (samples). Relationships among the selected samples were also assessed based on data obtained from a wider polyphenol identification performed without chemical standards using a multiple factorial analysis (MFA). The methodology of the MFA included data transformation ($\ln(x+1)$); then, compounds were grouped into classes and data were reported as observations and variables maps. Vector lengths and directions reported in the variable maps are directly correlated to their significance within each compound class. Results are reported in Supplemental information (Fig. S6). PCA and MFA computations were performed using XLSTAT (version 2016.02.27444).

Table 1
List of polyphenolic compounds from olive leaves identified and quantified in leaf samples by HPLC DAD ESI/MS-TOF using specific chemical standards.

Compound	RT (min)[a]	$(M-H)^-$	*m/z* Exp[b]	*m/z* Clc[c]	Δm (ppm)[d]	Score[e]	Reference
Quinic acid	0.469	$C_7H_{11}O_6$	191.0567	191.0609	-2.96	93.23	(Taamalli et al., 2013; Talhaoui et al., 2014)
Hydroxytyrosol glucoside	1.025	$C_{14}H_{19}O_8$	315.1098	315.1085	-3.94	84.88	(Taamalli et al., 2013; Talhaoui et al., 2014)
Rutin	6.069	$C_{27}H_{29}O_{16}$	609.1467	609.1461	-1.00	79.33	(Fu et al., 2010; Talhaoui et al., 2015)
Quercetin glucoside	6.290	$C_{21}H_{19}O_{12}$	463.0898	463.0882	-3.42	76.49	(Talhaoui et al., 2014; Fu et al., 2010; Talhaoui et al., 2015; Quirantes-Piné et al., 2013)
Luteolin 7-O glucoside	6.432	$C_{21}H_{19}O_{11}$	447.0932	447.0933	0.23	88.75	(Fu et al., 2010; Taamalli et al., 2012)
Verbascoside	6.993	$C_{29}H_{35}O_{15}$	623.1985	623.1981	-0.64	77.09	(Lozano-Sánchez et al., 2010; Talhaoui et al., 2015)
Oleuropein	8.829	$C_{25}H_{31}O_{13}$	539.1791	539.1770	-3.92	58.69	(Lozano-Sánchez et al., 2010; Taamalli et al., 2013; Talhaoui et al., 2014)
Luteolin	11.939	$C_{15}H_9O_6$	285.0419	285.0455	-4.87	97.08	(Lozano-Sánchez et al., 2010; Taamalli et al., 2013)

[a] Retention time,
[b] *m/z* experimental,
[c] *m/z* calculated,
[d] difference between the observed mass and the theoretical mass of the compound (ppm),
[e] isotopic abundance distribution match: a measure of the probability that the distribution of isotope abundance ratios calculated for the formula matches the measured data. *Compound positively identified with authentic chemical standards

3. Results

3.1. Morphological and physiological results

3.1.1. Biometric data

Salinity treatments negatively affected the fresh weight (FW) of leaves in all cultivars, except for LA, in which no significant changes appeared between the different treatments (Fig. 1A).

Two-way ANOVA analyses indicated that both experimental factors (i.e., cultivar and treatment) and their interaction were statistically significant. For OL, post-test analyses indicated a drop in leaf FW of 44% and 72% at 100 mM and 200 mM NaCl, respectively, compared with control, and in LE, a decrease of 33% and 52% at 100 mM and 200 mM, respectively. In contrast, FR showed a significant reduction (35%) in leaf FW only at 200 mM NaCl. We observed cultivar-dependent differences in root FW (Fig. 1B), but no differences in stem FW (Fig. 1C). The FW of the whole plant (Fig. 1D) was both cultivar- and treatment-dependent. However, only LE showed a significant decrease (27% and 34%) at 100 mM and 200 mM NaCl, respectively, compared with control. Supplemental information reports data related to analyses on fresh (FW) (Table S1) and dried (DW) plant material (Table S2); in the latter case, no significant changes were found for stem, root and total biomass, while salinity negatively reduced the leaf DW in LE and OL only.

3.1.2. Photosynthetic data

Photosynthetic parameters were evaluated weekly for eight weeks using a portable gas exchange measuring system. There was a negative cumulative effect at the end of the trial on gas exchange parameters in all cultivars due to salinity treatment (Fig. 2). Supplemental information shows the time-course data (Figs. S2-S5). The net carbon assimilation rate (A_n) decreased after salt treatments in all the cultivars (Fig. 2A) but did not differ between the two levels of NaCl. The greatest proportional decline was found in FR, in which assimilation rates were reduced by 60% in both 100 and 200 mM NaCl. The most significant differences among cultivars were evident in the moderate (100 mM) NaCl treatment. Reductions in stomatal conductance rates (g_s) followed the same pattern, with FR again showing the greatest reduction (35%) among the four cultivars (Fig. 2B). In all remaining cultivars, g_s declined by 10–20% in the salinity treatments, with the smallest change in LE between salinity-stressed and control plants. The average intercellular CO_2 concentrations (C_i) increased with both NaCl concentrations, showing inverse trends relative to the carbon assimilation rates (Fig. 2C) and the greatest increase in the cultivars LA and LE. The function of the PSII light harvesting complexes were not strongly affected by salinity treatments. Maximum quantum yield (Fv/Fm) values were stable following eight weeks of treatment, regardless of the salt concentration (Fig. 2D). Surprisingly, slightly significant increases were observed in FR plants treated with 200 mM NaCl as well as in OL in both 100 and 200 mM NaCl, compared to controls. In contrast, 100 mM NaCl had a negative

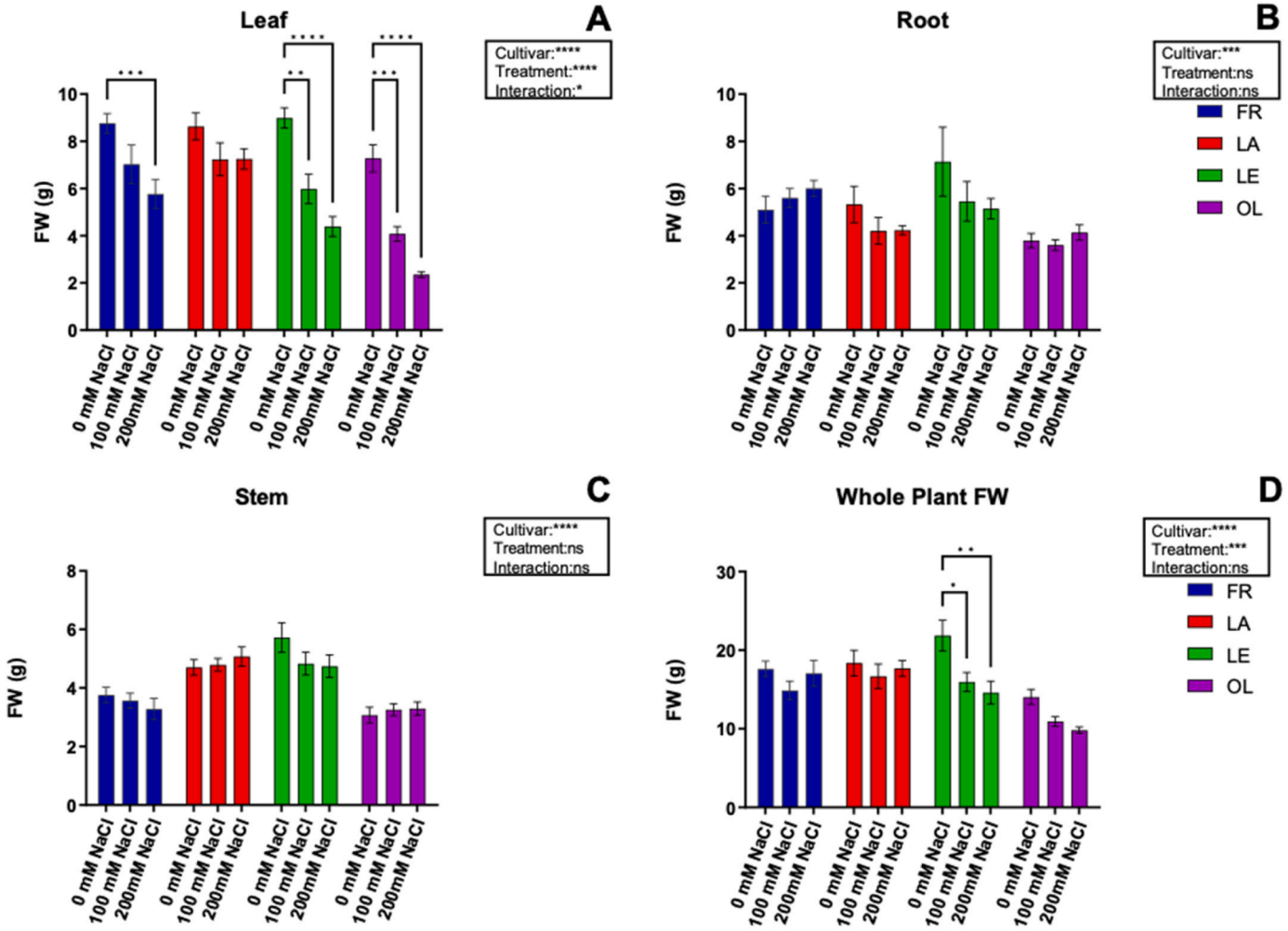

Fig. 1. Fresh weight (FW) data of different tissues (leaf, root, stem) from four olive cultivars (FR, LA, LE, OL) subjected to different saline irrigation. Tukey-HSD was performed as two-way ANOVA post hoc test according to the cultivar variable. * ** * < 0.0001 * ** < 0.001 * * < 0.01 * < 0.05. Data were reported as mean ± S.E. M. (n = 10).

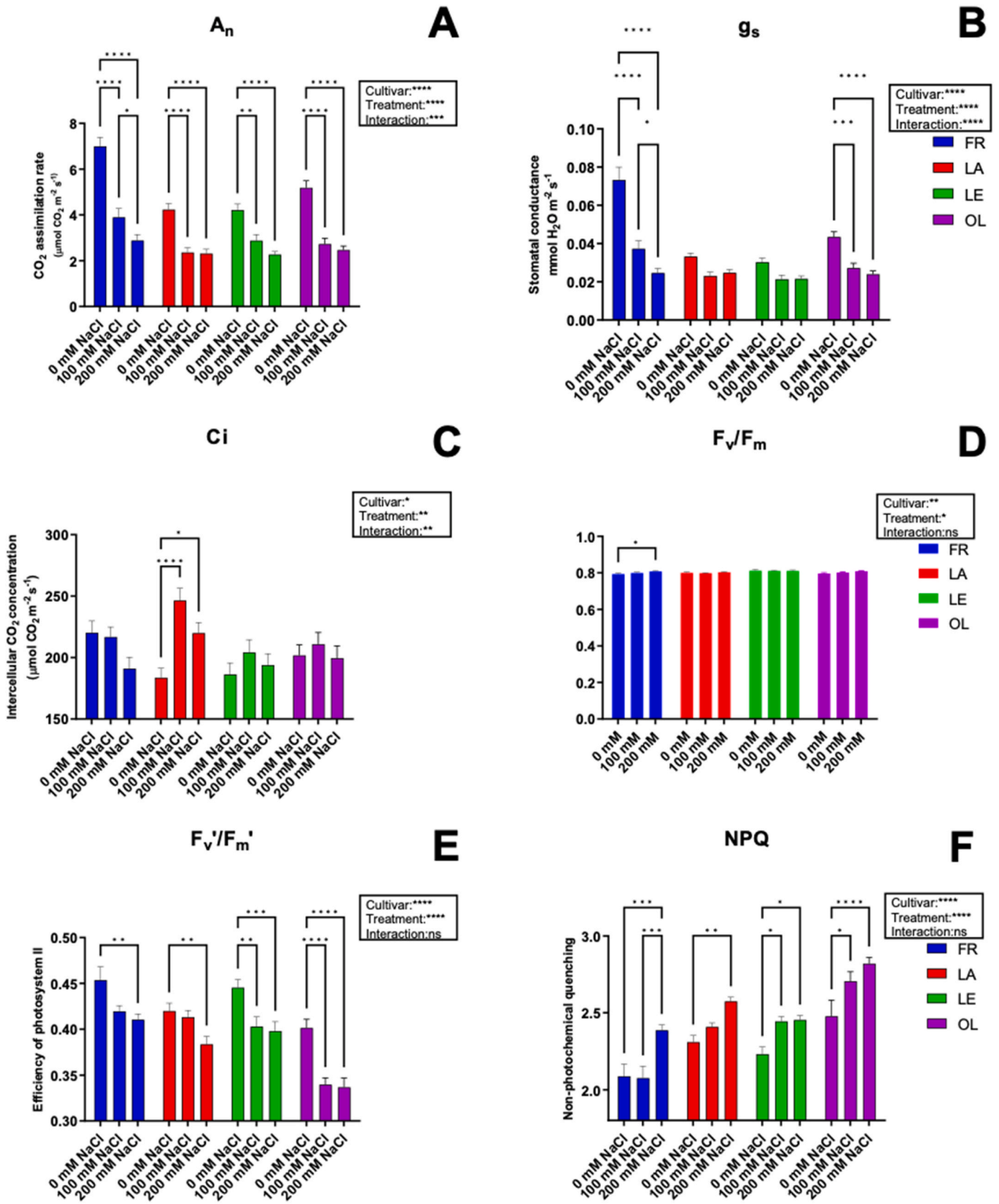

Fig. 2. Net carbon assimilation rate (A_n), stomatal conductance (g_s), intercellular CO_2 concentration (C_i), non-photochemical quenching (NPQ), maximum quantum yield (Fv/Fm) and the efficiency of photosystem II (F_v'/F_m') of four olive cultivars (FR, LA, LE, OL) subjected to different saline irrigation. All values are presented as mean value ± S.E.M. (n = 40 for A_n, g_s, C_i; n = 24 for NPQ, Fv/Fm and Fv'/Fm'. Statistical significance of the difference between control and salinity-stressed leaves was assessed by two-way ANOVA and Tukey HSD post hoc test (p-value <0.05). * *** * < 0.0001 * ** < 0.001 * * < 0.01 * < 0.05.

effect on the effective quantum yield (F_v'/F_m') values of all four cultivars, with significant changes observed in LE and OL (Fig. 2E), but the decline was not exacerbated by 200 mM NaCl and values for FR and LE were similar to those of control plants. Increasing salt concentrations resulted in augmented NPQ values, with significant changes observed in FR, LA, and LE treated with 200 mM NaCl, compared to controls (Fig. 2F). In OL, values were similar across all treatments.

3.2. Results of ion measurements

Sodium and potassium concentrations were measured in leaf, stem, and root tissues at the end of eight weeks (Fig. 3, Table S3). Raw data were used to calculate K^+/Na^+ ratios (Table S4). The accumulation and translocation of sodium into all tissues for all cultivars was correlated with the salt concentration (Fig. 3A, D and G). The highest Na^+ concentration change in all cultivars was measured in roots, followed by stems and leaves. The highest Na^+ concentration changes in leaves were measured in 200 mM NaCl-treated plants of LE and OL, compared to FR and LA. In stems (Fig. 3D), Na^+ concentrations also varied significantly in all cultivars, compared with controls, with OL and LA exhibiting the greatest Na^+ concentration changes in both 100 mM and 200 mM NaCl treated plants. In roots (Fig. 3G), Na^+ concentrations of plants treated with 200 mM NaCl ranged from 25.1 to 29.3 mg g^{-1} DW, with LE exhibiting the highest amount of Na^+, followed by LA, FR and OL. Salinity affected tissue potassium concentrations in a dose- and tissue-dependent manner, lowering K^+ concentrations in all tissues (Fig. 3B, E and H; Table S3). The highest K^+ concentration values were measured in leaves of control plants (Fig. 3B) and decreased in all tissues with exposure to salinity stress in all cultivars and treatments. In leaves, a 1.3-fold decline occurred in OL, while a 1.23-, 1.2- and 1.2-fold decrease was observed in FR, LE and LA, respectively. Variations were particularly evident in the stems of FR and LA (Fig. 3E). Salinity induced a significant cultivar-dependent decline in root K^+ concentrations (Fig. 3H): in FR, a dramatic (3-fold) reduction was observed at 200 mM NaCl, compared to control, while in LA, LE and OL the corresponding decrease was about 1.5–2-fold. 100 mM and 200 mM NaCl significantly reduced K^+/Na^+ ratios in all olive cultivars (Fig. 3C, F, and IG). Surprisingly, at 200 mM NaCl, FR was the only cultivar with a leaf K^+/Na^+ ratio > 1 (Fig. 3C,

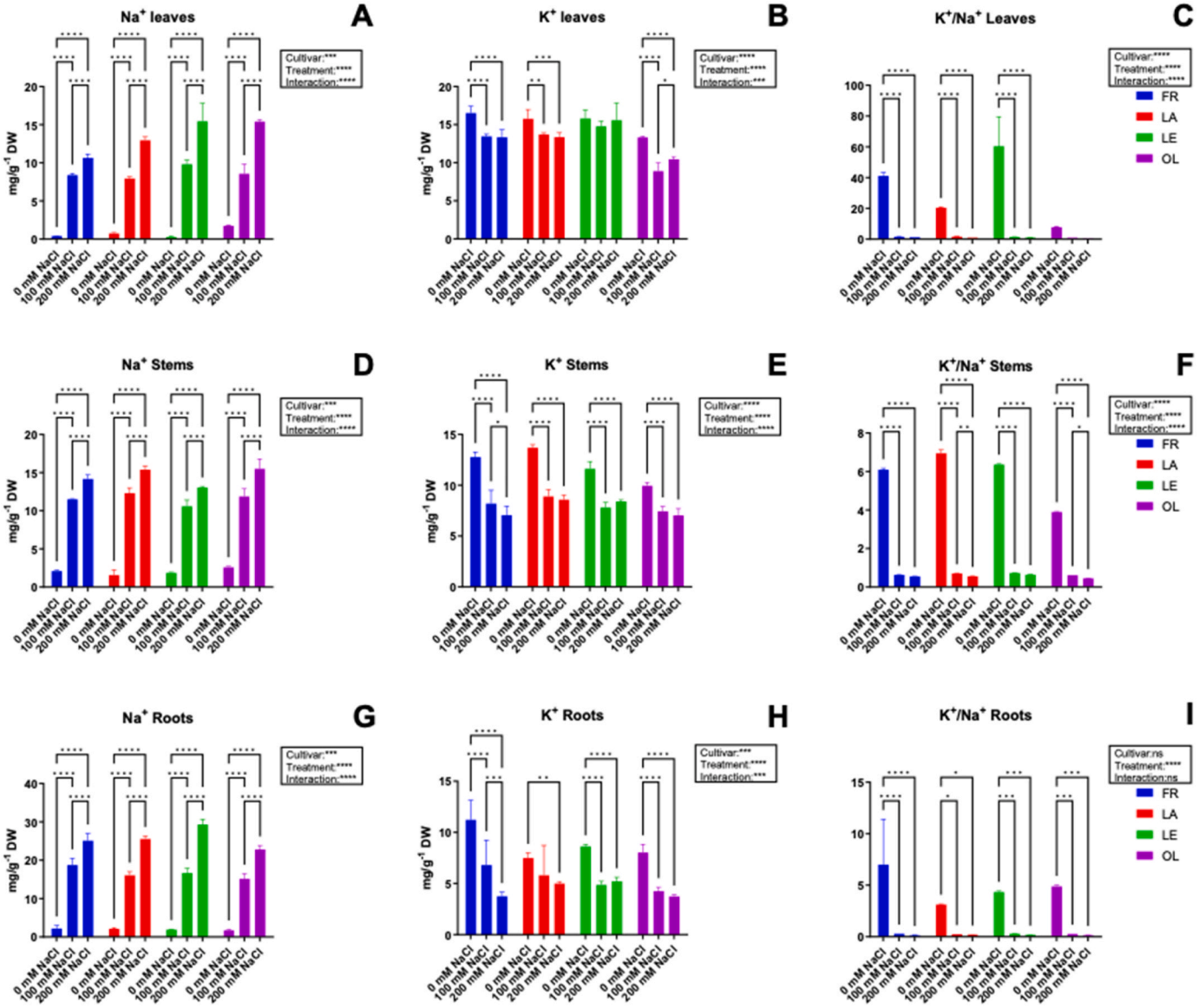

Fig. 3. Na^+ and K^+ concentration, and K^+/Na^+ ratio values measured in different plant tissues (leaf, stem, root) of four olive cultivars (FR, LA, LE, OL) subjected to different saline irrigation. (*A-C*) Leaf data. (D-F) Stem data. (G-I) Root data. Statistical evaluation of data was performed according to two-way ANOVA coupled with Tukey test (p-value <0.05). Values are mean ± S.E.M. (n = 6). * *** * < 0.0001 * ** < 0.001 * * < 0.01 * < 0.05.

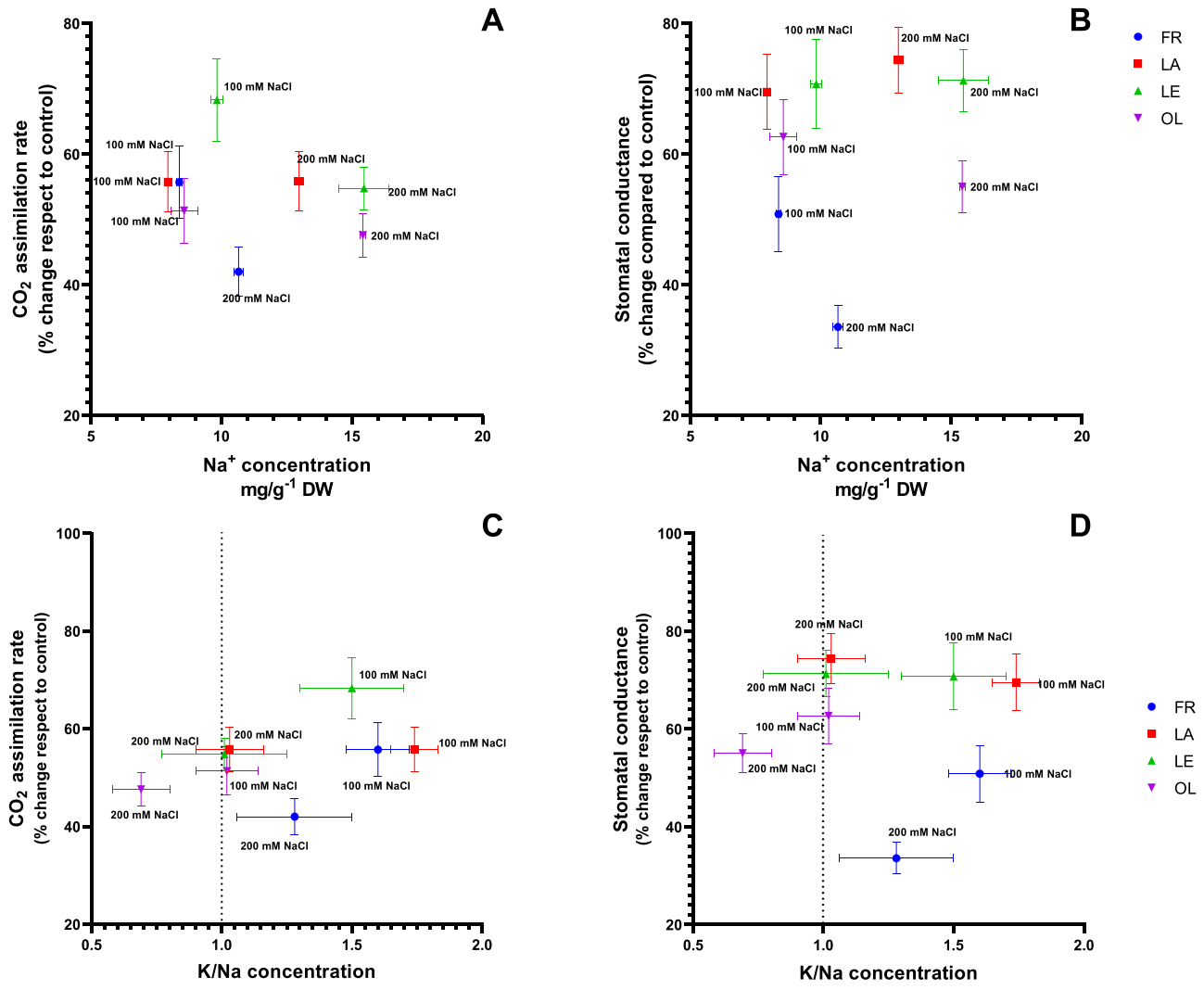

Fig. 4. Relationships occurring between ion and photosynthetic data in four olive cultivars (FR, LA, LE, OL) subjected to different saline irrigation. Data describing the relationship between the K^+/Na^+ value inside the leaves after eight weeks of the experiment with net carbon assimilation rate (A_n) (*A*, upper, left) and stomatal conductance (g_s) (*B*, upper right). The dotted line indicates a condition in which the K^+/Na^+ value is equal to one. Results are related to data comparison between leaf Na^+ content after eight weeks and carbon assimilation rate (*C*, bottom, left) or stomatal conductance (*D*, bottom, right), respectively. Symbols represent the different cultivars, as shown in the legend. All values are presented as mean value ± S.E.M. (n = 40 for A_n and g_s, n = 6 for ion content). * ** * < 0.0001 * ** < 0.001 * * < 0.01 * < 0.05.

Table S4), while LE had the greatest values for this parameter in stem (Fig. 3F) and root (Fig. 3G).

Salt treatments caused similar, significant variations in all cultivars that was not dose-dependent. Conversely, significant genotype-dependent differences were measured in leaf, stem and root K^+/Na^+ ratio values of control plants.

Sodium accumulation in leaves were correlated with carbon assimilation rates (A_n) and stomatal conductance (g_s), expressed as % change in treated samples (100 mM and 200 mM NaCl), compared with control (Fig. 4). Moreover, A_n and g_s results were also correlated with calculated K^+/Na^+ values. FR was the only cultivar that maintained a positive K^+/Na^+ ratio at 200 mM NaCl, despite a considerable decrease in photosynthetic parameters; conversely, the other cultivars showed a negative K^+/Na^+ value at 200 mM NaCl, but their photosynthetic parameters were not negatively affected.

3.3. Identification and quantification of polyphenolic compounds

The metabolomic analysis of leaves collected after eight weeks of exposure to salinity led to the identification of eight different compounds (Fig. 5). The effect of salinity stress on the polyphenolic profiles of all four cultivars was assessed through a metabolomic analysis of leaves collected after eight weeks. Polyphenolics were determined first by HPLC ESI/MS-TOF using appropriate standards (Fig. 5), and then without standards (Table S5) as a method to identify a wider range of compounds. Retention times, experimental and calculated *m/z* values, and molecular formulas of phenolic compounds identified through chemical standards are reported in Table 1. Eight different compounds were identified and quantified (Fig. 5).

Quinic acid levels of FR, LA, LE and OL treated plants indicated that salt drastically reduced the concentration of this polyphenol in each cultivar in a dose-dependent manner (Fig. 5A). In the case of rutin, FR and LA showed increased concentrations due to treatments with 200 mM and 100 mM, respectively, with respect to control (Fig. 5B). Conversely, a significant decrease in rutin concentration was measured in LE in both 100 and 200 mM NaCl, and no change in OL. A two-way ANOVA indicated that the treatment level and interaction effects were more significant than cultivar. LA exhibited a significant increase in verbascoside concentration in both treatments, while in LE it was only evident with 200 mM NaCl (Fig. 5C). Conversely, FR and OL maintained

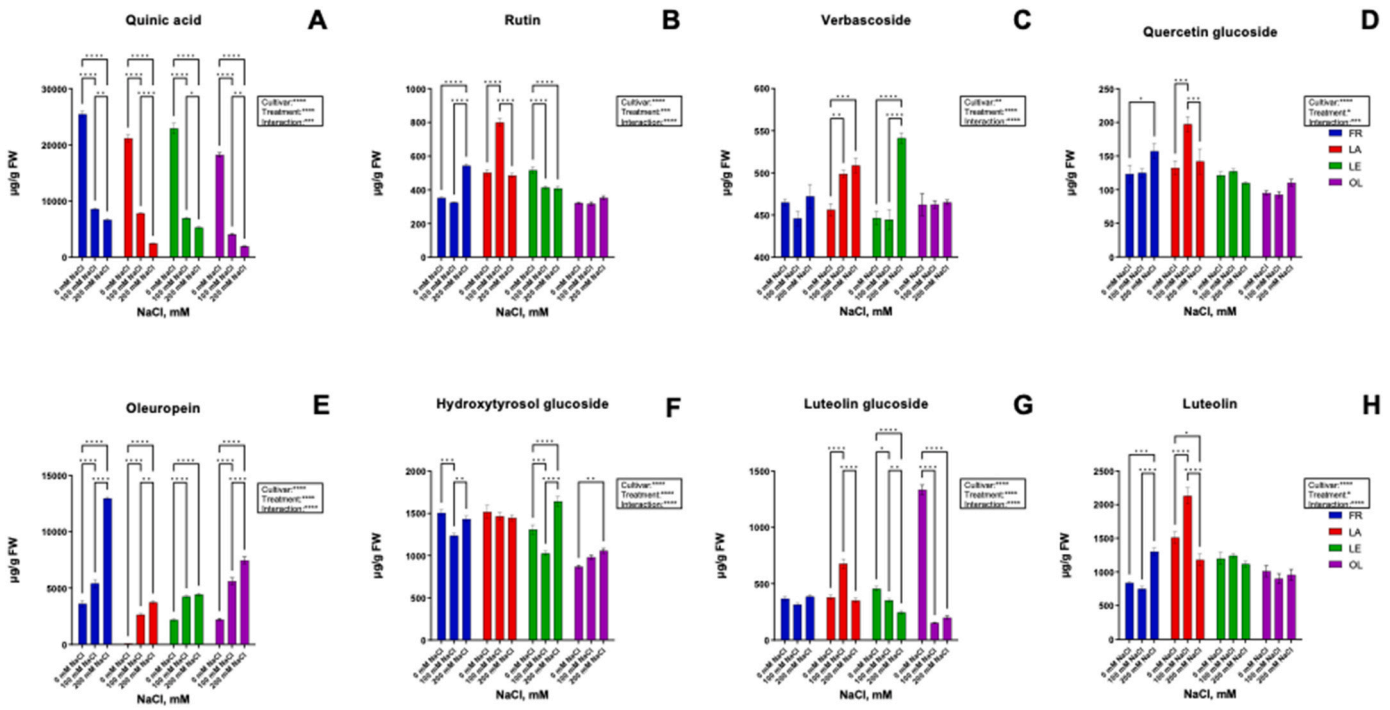

Fig. 5. HPLC-DAD ESI-MS results of the main polyphenolics identified in olive leaves using reference standard compounds. *(A-H)* Two-way ANOVA coupled with Tukey test (p-value <0.05) was performed. Values are mean ± S.E.M. (n = 3). * ** * < 0.0001 * ** < 0.001 * * < 0.01 * < 0.05.

stable verbascoside concentrations after salinity treatment. While no significant changes in quercitin glucoside due to salinity treatments were observed in LE and OL (Fig. 5D), an appreciable increase in quercetin concentration occurred in FR with 200 mM NaCl, and in LA with 100 mM NaCl. Irrigation with different NaCl concentrations increased the oleuropein concentrations in all cultivars in a dose-dependent manner (Fig. 5E), with the greatest increase occurring in FR. Hydroxytyrosol glucoside levels changed significantly after salinity treatments in FR, LE and OL (Fig. 5F). A significant decrease occurred in FR with 100 mM NaCl, compared with control, and a significant reduction and increase was observed in LE with 100 mM NaCl and 200 mM NaCl, respectively. Luteolin glucoside levels varied due to the treatment (Fig. 5G); they decreased in both OL and LE with both 100 mM NaCl and 200 mM NaCl, compared to control. In LA, an evident increase was observed only with 100 mM NaCl. Lastly, luteolin levels significantly increased after salt irrigation in FR and LA (Fig. 5H); conversely, no significant changes occurred in LE or OL. A pronounced increase in luteolin concentration was observed in FR with 200 mM NaCl, while this increment occurred in LA only with 100 mM NaCl.

Principal component analysis (PCA) performed on polyphenolic data (Table 1) showed that the first two dimensions (F1, F2) accounted for 64.85% of the total variance of the system, with the first (F1) and the second (F2) axis explaining 39.80% and 25.05%, respectively (Fig. 6).

Looking at sample distribution (Fig. 6A), controls were usually placed in lower quadrants of the PCA; conversely, treated samples were mostly placed in the upper quadrants, effectively grouping the samples based on cultivar (F1) and treatment (F2). Furthermore, no significant differences were observed in OL between 100 mM and 200 mM NaCl-treated plants, whereas the treatment groups were clustered separately in different quadrants for FR and LE. From this perspective, the most significant differences occurred with LA and FR samples, with 100 mM and 200 mM, clearly separated according to F1, the axis that explains the higher variance of the dataset. The variable map highlights the correlation among compounds (Fig. 6B). Data indicate that quercetin glucoside, rutin and luteolin were positively correlated with F1. Rutin, the most significant compound based on vector length, was positively correlated with quercetin glucoside and hydroxytyrosol glucoside. In contrast, it was negatively correlated with oleuropein. The latter compound showed a general negative correlation with most of the polyphenols identified through standards.

The pool of metabolites identified without using standards (Table S5) was used to compute MFA analysis by grouping polyphenols in eight functional classes and accounting for 44.65% of the total variance of the dataset (28.75%, F1; 15.90%, F2). Data reported in Fig. S6A indicate that samples were clearly separated based on treatments, with control samples placed in the left quadrants, whereas treated samples were mostly placed in the right quadrants. Looking at the contribution of compound classes according to MFA (Fig. S6B), it was observed that unknown and secoiridoid classes mainly contributed to PC1, whereas flavonol, sugar, lignan and flavonoid ones contributed to PC2. Lastly, flavonol and flavonoid classes contributed most to PCA as indicated by vector lengths reported in Fig S6C.

3.4. Proteomic results

Quantitative TMT-based proteomic experiments on leaf samples were performed to depict the general and cultivar-dependent molecular response of olive plants to salinity stress. Accordingly, a pairwise comparison was separately performed for each cultivar (FR, LA, LE, OL) by comparing the stress condition (200 mM NaCl) with the control (0 mM NaCl). Mass spectrometry analyses identified 1765 non-redundant proteins using the threshold parameters reported in the experimental section. Within this dataset, 410 proteins were further selected according to both p-value (<0.05) and fold change (>2.0, overrepresented; <0.5, downrepresented) values, assigning differentially represented proteins (DRPs) (Dataset S1). Most of these DRPs were identified in stress vs control comparisons of FR and LE, with 234 (190 overrepresented, 44 downrepresented) and 213 proteins (150 overrepresented, 63 downrepresented), respectively. A different picture was observed for LA and OL, which displayed a lower number of DRPs in response to salt stress, i.e., 27 (12 overrepresented and 15 downrepresented) and 57 (33 overrepresented and 24 downrepresented), respectively.

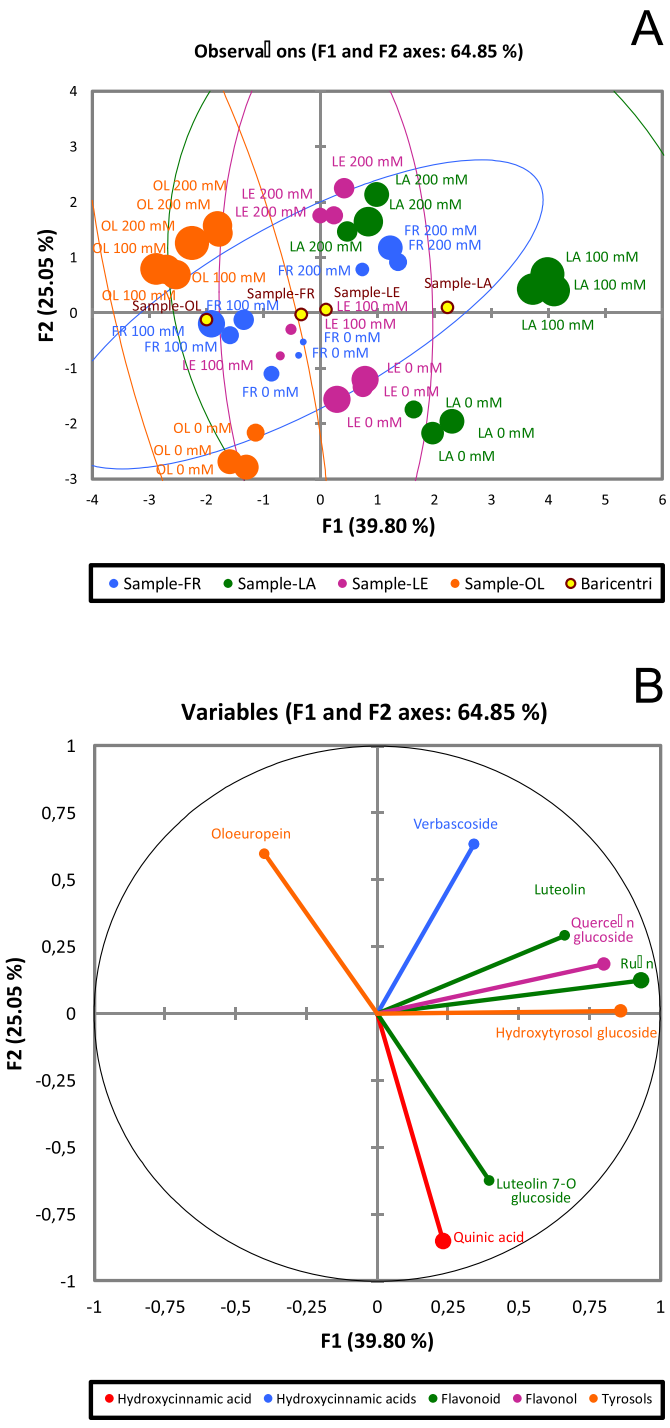

Fig. 6. Principal component analysis (PCA) of polyphenolic compounds identified in olive leaves using reference standard compounds. (*A*) According to results from multifactorial analysis, the observation factor map linked to the sample distribution. (*B*) Variable factor map related to the contribution of each polyphenol compound in the sample distribution. The length of the vectors is correlated to their significance. The angle α formed between two vectors, or between a vector and an axis, indicates a positive correlation for $0 \leq \alpha < 90°$ (*r* close to 1), a negative correlation for $90° < \alpha \leq 180°$ (*r* close to −1), and no linear dependence for $\alpha = 90°$ (*r* close to 0). PC1, first dimension; PC2, second dimension.

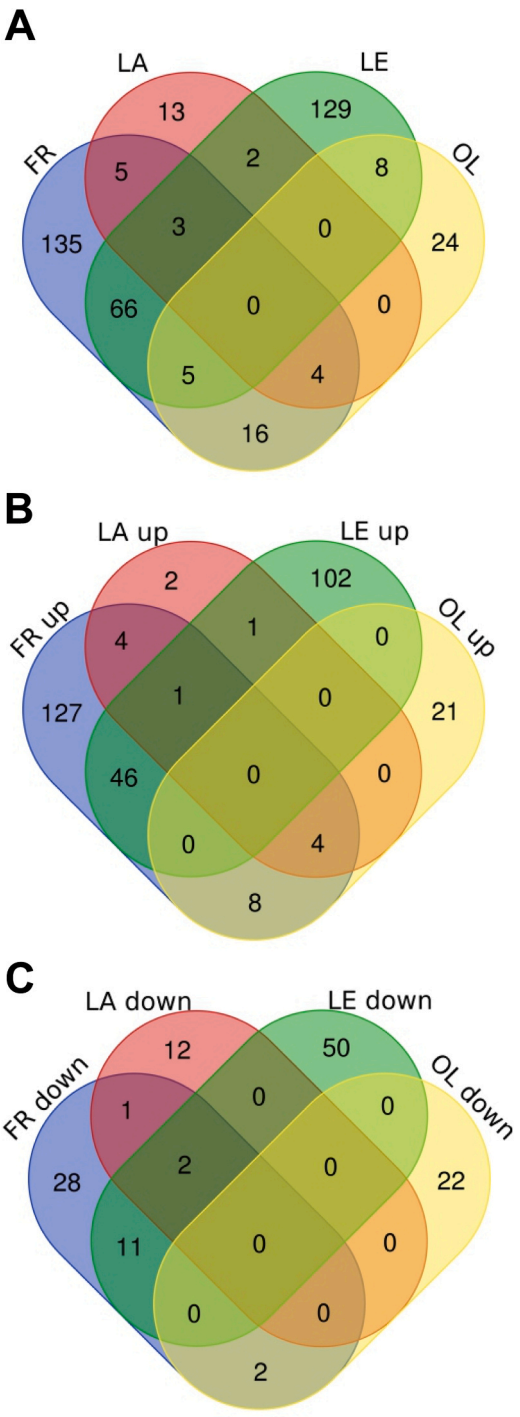

Fig. 7. Venn diagrams of differentially represented proteins in olive leaves (*p*-value <0.05; fold change > 2.0) as observed in salinity stressed vs control comparisons of four cultivars (FR, LA, LE, OL) subjected to saline irrigation. (*A*) Data are related to the sum of overrepresented and downrepresented proteins (FR=234, LE=213, LA=27, OL=57). (*B*) Overrepresented (FR=190, LE=150, LA=12, Oliana=33) and (*C*) downrepresented proteins (FR=44, LE=63, LA=15, OL=24). FR=Frantoio, LE=Leccino, LA=Lecciana, OL=Oliana.

Venn diagrams were generated for DRPs to assess the overall effect of salinity in each cultivar (Fig. 7A), with a focus on overrepresented (Fig. 7B) and downrepresented (Fig. 7C) proteins. They indicated that most DRPs were cultivar-dependent, with no proteins shared by all the ecotypes. The highest number of DRPs shared by cultivars occurred in FR and LE, which had 47 overrepresented and 13 downrepresented

proteins in common. A general comparison of the DRPs reported in Figs. 7B and 7C showed that salt irrigation mostly induced more overrepresented (316) than downrepresented (128) proteins. In terms of unique overrepresented proteins, FR and LE exhibited the highest number of DRPs (127 and 102, respectively), whereas OL and LA showed only 21 and 2 DRPs, respectively (Fig. 7B). In terms of unique downrepresented proteins, LE showed the highest number of DRPs (50), followed by FR (28), OL (22), and LA (12).

All DRPs were then indexed by an automatic functional assignment and the results were further integrated with information from recent scientific literature. DRPs identified from different plant protein databases were at first analyzed by BLAST to assign specific *Arabidopsis thaliana* orthologs from TAIR database; then, corresponding codes were used for functional analysis (Dataset S2 and S3). Accordingly, most of the proteins were associated with one or two function(s), while 8% remained unassigned. Fold change (FC) values were also calculated according to a $\log_2$ basis (Dataset S3; Table S6), estimating that quantitative variations among top overrepresented and top downrepresented proteins were higher in LE ($\Delta\log_2$ =9.96) and FR ($\Delta\log_2$ =7.68), with respect to OL ($\Delta\log_2$ =5.05) and LA ($\Delta\log_2$ =4.39), once again highlighting the lower proteomic response in the latter two cultivars after salt irrigation.

All overrepresented proteins in FR were mostly related to photosynthetic activity (38%) and protein degradation and carbohydrate metabolism (7%) (Fig. S7A). Among the proteins showing the highest levels of overrepresentation are serine/threonine-protein phosphatase (PP2A) (AT3G58500.1) ($\log_2$FC 4.21), D2 protein in the reaction center of PS II (ATCG00270.1) ($\log_2$FC 3.1), and a specific ferredoxin-$NADP^+$-oxidoreductase (AT1G20020.1) ($\log_2$FC 3.06) (Dataset S2; Table S6). In FR, downrepresented proteins were primarily associated with protein degradation (23%) and external stimuli response (13%) (Fig. S7B). The three most downrepresented proteins were a carboxylesterase linked to salicylic acid production (AT2G23620.1) ($\log_2$FC −3.47), a neutral ceramidase involved in responses to oxidative stress (AT1G07380.1) ($\log_2$FC −2.99), and a germin-like auxin-binding protein (AT5G20630.1) ($\log_2$FC −2.99) (Dataset S2; Table S6).

Regarding LA, overrepresented proteins included components related to photosynthesis (62%) and protein biosynthesis or not assigned (15%) (Fig. S8A). The three most overrepresented proteins were chlorophyll a-b binding proteins 3 (AT5G54270.1) ($\log_2$FC 1.95) and LHCII type 1-like (AT2G34430.1) ($\log_2$FC 1.59), and chloroplastic ATP synthase subunit beta (ATCG00480.1) ($\log_2$FC 1.58) (Dataset S2; Table S6). In LA, downrepresented proteins were mostly related to protein degradation (19%) and carbohydrate metabolism or secondary metabolism (14%) (Fig. S8B). The three most downrepresented proteins were two isoforms of beta-glycosidase (AT5G44640.1) ($\log_2$FC −2.44 and −1.97), and lipoxygenase (AT1G17420.1) ($\log_2$FC −2.27) (Dataset S2; Table S6).

In LE, overrepresented proteins were mainly related to photosynthetic activity (27%) and protein degradation (12%) (Fig. S9A). The three most overrepresented proteins were ubiquinol-cytochrome C reductase (AT3G52730) ($\log_2$FC 4.73), D2 protein in the reaction center of PS II (ATCG00270.1) ($\log_2$FC 4.7), and dirigent-like protein (AT5G42510.1) ($\log_2$FC 4.67) (Dataset S2; Table S6). In LE, downrepresented proteins were associated with photosynthesis (21%) and no known function (18%) (Fig. S9B). Those showing the lowest levels of downrepresentation were a polypeptide found in the chloroplast stroma involved in the Calvin cycle (AT3G62410.1) ($\log_2$FC −5.23), glycine carboxylase (AT1G32470.1) ($\log_2$FC −4.34), PSI type III chlorophyll a/b-binding protein (AT1G61520.3) ($\log_2$FC −4.2) and late embryogenesis abundant protein ATEM6 (AT2G40170.1) ($\log_2$FC −3.35) (Dataset S2; Table S6).

Overrepresented proteins in OL mostly included components related to photosynthesis (64%) and cell wall organization (15%) (Fig. S10A). The top three overrepresented proteins in OL were a plastocyanin-like protein (AT1G76100.1) ($\log_2$FC 2.21), light-harvesting chlorophyll a/b binding protein (AT4G10340.1) ($\log_2$FC 1.77), and a subunit of the light-harvesting complex II (AT1G29930.1) ($\log_2$FC 1.71). In OL, downrepresented proteins were related to photosynthesis (36%) and protein biosynthesis (18%) (Fig. S10B). Two of the top three downrepresented proteins in OL ($\log_2$FC −2.84 and −2.69) have no orthologs in *Arabidopsis thaliana* according to the TAIR database and were not functionally assigned; they were assigned as globulin-like and glutenin components. The third is a tyrosine-phosphorylated protein that is also a large unit of rubisco (ATCG00490.1) ($\log_2$FC −1.9).

Data reported above suggested that the functional categories (and the corresponding percentage values) associated with DRPs related to salinity irrigation were roughly similar in all olive cultivars, but the number and, more importantly, the nature and the quantitative levels of the differentially represented proteins varied considerably depending on the ecotype (Dataset S1-S3). This condition is well represented in Table 2, in which DRPs were grouped to identify common variably represented proteins in various cultivars that simultaneously bear at the same time a p-value < 0.05 and a $\log_2$ fold-change value ≥ 1.5 or ≤ -1.5 in at least two ecotypes. In this context, we recognized 8 proteins as deregulated in three accessions after salinity stress: i) beta-glucosidase (AT5G44640.1), which was downrepresented in FR, LA and LE; ii) five ribulose-1,5-bisphosphate carboxylase/oxygenase isoforms, which were at the same time overrepresented in FR and LE, and downrepresented in OL; iii) photosystem II 22 kDa protein (AT1G44575.1) and plastocyanin-like protein (AT1G76100.1), which were simultaneously overrepresented in FR and OL, and downrepresented in LE (Table 2). Notwithstanding their quantitative trend, most of the proteins reported in Table 2 were associated with photosynthetic activity, with overrepresented components that were always higher in number than corresponding downrepresented counterparts.

3.5. Gene-ontology analysis of DRPs highlights specific metabolic components involved in plant response to salinity stress

3.5.1. Overrepresented proteins in the four olive cultivars

The gene-ontology map showed that overrepresented DRPs in FR involved in *Biological processes* were mainly linked to metabolic processes, such as photosynthesis, energy production and response to stimuli (Fig. S11). Photosynthesis and energy were linked to many proteins related to organophosphate, glucosyl, and purine metabolic processes. These, in turn, were strictly associated with nucleoside and nucleoside phosphate metabolism, both of which were connected to purine metabolism and ATP metabolic process. On the other hand, a mild overrepresentation of specific proteins involved in abiotic stress was also observed in FR. Concerning *Molecular function*, the main overrepresented proteins were related to antioxidants, structural molecules, transport activity, binding, and catalytic activity. In particular, the binding function was highly up-regulated for tetrapyrrole and chlorophyll; transport activity was slightly overrepresented for monovalent inorganic cation and hydrogen transmembrane transported components. Lastly, *Cellular components* implicated in stress in FR were the chloroplast and mitochondria. In particular, the highest number of overrepresented proteins were connected to the chloroplast lumen and membrane, affecting both photosystems (photosystem I less than photosystem II). Accordingly, the mitochondrial membrane seemed to be implicated in salt stress response to a lower extent than chloroplasts.

As described above, the number of overrepresented DRPs in LA was limited to 13. They were mainly linked to cellular and metabolic processes, such as photosynthesis and organonitrogen compounds (Fig. S12). The limited number of overrepresented proteins did not allow for the specification of gene ontology relative to *Molecular function*, but in terms of *Cellular components,* they were primarily linked to chloroplast and membrane protein complexes.

As shown in Fig. S13, *Biological processes* of overrepresented DRPs in LE were strictly linked to cellular metabolic processes, namely photosynthesis and the generation of precursor metabolites and energy, and

Table 2
Selected DRPs commonly identified in salt stressed vs control pairwise comparisons of four olive cultivars (FR, LA, LE, OL) subjected to different saline irrigation.

Functional classification	AGI code*	Description	Accession Number**	(FR 200 mM salt) / (FR Ctrl)	(LA 200 mM salt) / (LA Ctrl)	(LE 200 mM salt) / (LE Ctrl)	(OL 200 mM salt) / (OL Ctrl)
Carbohydrate metabolism	*AT1G66430.1*	Probable fructokinase-6, chloroplastic [*O. europaea* var. sylvestris]	1278993096	**2.3**	0.97	**2.26**	0.83
Carbohydrate metabolism	*AT5G44640.1*	Beta-glucosidase [*O. europaea* var. sylvestris]	1279053867	**-2.09**	**-2.44**	**-2.21**	0.25
Carbohydrate metabolism	*AT3G57240.1*	Glucan endo-1,3-beta-glucosidase, acidic-like [*O. europaea* var. sylvestris]	1279067887	**2.63**	0.93	**1.68**	-0.18
Cellular respiration	*AT4G34700.1*	NADH dehydrogenase [ubiquinone] 1 beta subcomplex subunit 9 [*O. europaea* var. sylvestris]	1279072963	**1.68**	0.48	**1.9**	-0.26
External stimuli response	*not assigned*	OE6A032615P1	OE6A032615P1	**-2.03**	-0.62	**-3.29**	0.3
External stimuli response	*AT5G25610.1*	BURP domain protein RD22-like [*O. europaea* var. sylvestris]	1279000809	**-2.85**	-0.69	**-1.5**	0.23
External stimuli response	*AT3G54420.1*	OE6A040457P1	OE6A040457P1	**-2.07**	-0.29	**-2.73**	0.03
Not assigned	*not assigned*	OE6A051559P1	OE6A051559P1	**-1.56**	-0.24	**-3.59**	0.59
Not assigned	*AT4G28940.1*	OE6A098060P2	OE6A098060P2	**2.64**	**0.85**	**1.82**	**0.56**
Not assigned	*ATCG00480.1*	AtpB, partial (chloroplast) [Cephaleuros sp. HZ-2017]	1409969998	**3**	**1.58**	1.05	0.41
Not assigned	*AT3G62410.1*	Calvin cycle protein CP12-1, chloroplastic [*Arachis duranensis*]	1012235069	**-1.58**	-0.25	**-5.23**	0.41
Not assigned	*not assigned*	Dehydrin DHN1-like [*O. europaea* var. sylvestris]	1278997625	**-2**	**-1.26**	**-1.98**	-0.75
Nucleotide metabolism	*AT5G18280.1*	OE6A073512P1	OE6A073512P1	**2.38**	-0.01	**1.87**	0.04
Nutrient uptake	*AT5G01600.1*	OE6A008047P3	OE6A008047P3	**2.24**	1.19	**1.68**	0.64
Photosynthesis	*AT1G76100.1*	Plastocyanin-like protein [*O. europaea* var. sylvestris]	1279038266	-0.4	0.37	**-3.43**	**2.21**
Photosynthesis	*AT1G31330.1*	Photosystem I reaction center subunit III, chloroplastic-like [*Papaver somniferum*]	1484791057	**1.82**	**1.21**	-6.64	**1.56**
Photosynthesis	*AT4G10340.1*	OE6A066649P3	OE6A066649P3	**1.09**	0.7	**-3.36**	**1.54**
Photosynthesis	*AT1G44575.1*	Photosystem II 22 kDa protein, chloroplastic [*O. europaea* var. sylvestris]	1279002304	**1.92**	1.04	-6.64	**1.52**
Photosynthesis	*AT3G14420.2*	Peroxisomal (S)-2-hydroxy-acid oxidase; glycolate oxidase [*Spinacia oleracea*]	121530	**2.27**	0.86		**1.5**
Photosynthesis	*AT3G14420.2*	OE6A100805P1	OE6A100805P1	**1.77**	0.66	**-2.11**	1.17
Photosynthesis	*AT2G34430.1*	Chlorophyll a-b binding protein of LHCII type 1-like [*Papaver somniferum*]	1484677501	**2.08**	**1.59**	0.6	**1.12**
Photosynthesis	*AT5G54270.1*	Chlorophyll a-b binding protein 3, chloroplastic [*Rosa chinensis*]	1365999475	**1.77**	**1.95**	0.95	1.07
Photosynthesis	*ATCG00270.1*	Photosystem II D2 protein, photosystem Q(A) protein [*Pisum sativum*]	29337172	**1.93**	0.62	**3.35**	0.77
Photosynthesis	*ATCG00720.1*	Cytochrome b6 [*Physcomitrium patens*]	61212625	**2.21**	0.9	**2.91**	0.7
Photosynthesis	*ATCG00270.1*	PSII D2 protein (chloroplast) [*O. europaea*]	283794963	**3.1**	0.6	**4.7**	0.65
Photosynthesis	*ATCG00280.1*	uncharacterized protein LOC111021989 [*Momordica charantia*]	1229801941	**2.22**	0.59	**2.88**	0.59
Photosynthesis	*ATCG00490.1*	Ribulose-1,5-bisphosphate carboxylase/oxygenase large subunit (chloroplast) [*Pseudochloris wilhelmii*]	723457465	**1.83**	0.62	**4.28**	0.03
Photosynthesis	*AT1G14150.1*	Photosynthetic NDH subunit of lumenal location 2, chloroplastic [*O. europaea* var. sylvestris]	1279040619	**1.81**	0.35	**1.73**	-0.11
Photosynthesis	*AT4G05180.1*	Oxygen-evolving enhancer protein 3, chloroplastic-like [*O. europaea* var. sylvestris]	1279107597	**1.52**	0.09	**1.68**	-0.12
Photosynthesis	*ATCG00020.1*	Photosystem II protein D1 (chloroplast) [*Pouteria campechiana*]	1134943990	**1.53**	0.06	**2.47**	-0.33
Photosynthesis	*ATCG00020.1*	Photosystem II protein D1, Photosystem II Q(B) protein [*Pleurastrum terricola*]	190360087	**1.77**	0.1	**1.77**	-0.35
Photosynthesis	*ATCG00490.1*	Ribulose-1,5-bisphosphate carboxylase/oxygenase large subunit, partial (chloroplast) [*Palhinhaea cernua*]	818945803	**2.39**	-0.09	**3.58**	-1.12
Photosynthesis	*ATCG00490.1*	Ribulose-1,5-bisphosphate carboxylase/oxygenase large subunit (chloroplast) [*Chionanthus retusus*]	1206249310	**1.8**	-0.52	**3.21**	-1.41
Photosynthesis	*ATCG00490.1*	Ribulose-1,5-bisphosphate carboxylase/oxygenase large subunit, partial (chloroplast) [*Spirogyra elongata*]	482515243	1.58	-0.87	**2.13**	**-1.71**
Photosynthesis	*ATCG00490.1*	Ribulose 1,5-bisphosphate carboxylase, partial (chloroplast) [*Davidsonia pruriens*]	17135922	**2.7**	-1	**2.99**	**-1.77**
Photosynthesis	*ATCG00490.1*	Ribulose-1,5-bisphosphate carboxylase dehydrogenase large subunit, partial (chloroplast) [*Plagiochila chauviniana*]	1127928349	**1.8**	-1.08	6.64	**-1.79**
Photosynthesis	*ATCG00490.1*	Ribulose-1,5-bisphosphate carboxylase/oxygenase large subunit (chloroplast) [*Burmeistera lutosa*]	1238899692	**1.83**	-0.52	1.59	**-1.84**
Photosynthesis	*ATCG00490.1*	Ribulose-1,5-bisphosphate carboxylase/oxygenase large subunit, partial (plastid) [*Capparis zeylanica*]	1209554793	**2.34**	-1.27	**2.77**	**-1.92**
Protein biosynthesis	*AT2G09990.1*	40S ribosomal protein S16-like [*Helianthus annuus*]	1228849965	**-2.58**	-0.63	-1.03	**-1.56**
Protein degradation	*AT5G07030.1*	Aspartyl protease AED3-like [*O. europaea* var. sylvestris]	1279071593	**-1.72**	-0.69	**-2.78**	0.44
Redox homeostasis	*AT3G26060.1*	Peroxiredoxin Q, chloroplastic [*O. europaea* var. sylvestris]	1279001800	**1.63**	0.38	**2.39**	0.14
Redox homeostasis	*AT4G35090.1*	OE6A048265P1	OE6A048265P1	**2.21**	0,15	**-2.12**	-0,54

Shown DRPs were selected based on the concomitant occurrence of a p-value < 0.05 and a $\log_2$ FC value ≥ 1.5 or ≤ -1.5 in at least two olive cultivars. In bold are reported data that were statistically significant, having a p-value < 0.05. Complete data are reported in Supplemental information (Dataset S1, S2 and S3, and Table S6). * = as result of BLAST analysis against TAIR (database 10);* *= Accession number of protein assigned by Proteome Discoverer (three databases).

the response to abiotic stimuli. Considering the *Molecular function* of overrepresented DRPs, a significant augmented regulation of catalytic activity principally related to hydrolase and peptidase activity was observed in LE, mostly related to the action of serine proteases, exopeptidases, and carboxypeptidases. Moreover, other overrepresented proteins were linked to antioxidants, electron carrier activity, and hydrogen ion transmembrane transport activity. Finally, *Cellular components* implicated in salinity stress in LE highlighted the prominent role of the chloroplast, as emphasized by the overrepresentation of proteins present in the thylakoid, stroma, and photosystem II.

Concerning *Biological* processes, several overrepresented DRPs in OL were linked to photosynthesis and response to abiotic stress (Fig. S14). The corresponding *Molecular function* was significantly connected to chlorophyll-binding. As with other cultivars, *Cellular components* of overrepresented proteins in OL were linked to chloroplast and membrane protein complexes.

3.5.2. Down-regulated proteins in FR and LE

The gene-ontology map showed that downrepresented DRPs implicated in salinity stress in FR were mainly involved in proteolysis (*Biological processes*) (Fig. S15). The corresponding *Molecular function* was related to the hydrolase activity, mostly linked to the action of peptidases. Regarding *Cellular components*, most downrepresented proteins were located around the external encapsulating structure, particularly the cell wall. Downrepresented DRPs in LE were largely involved in two *Biological processes*, namely the response to abiotic stimuli and photosynthesis (Fig. S16). As to *Molecular function*, a significant down-regulation of proteins related to hydrolase and peptidase activities was observed, and the downrepresented DRPs highlighted the prominent role of the chloroplast within *Cellular components*.

4. Discussion

In this study, an investigation into the effect of salt irrigation on the physiology of four different olive cultivars elucidated a variety of salinity-tolerance or -avoidance mechanisms. LE and OL exhibited lower fresh weight values than LA and FR, indicating a reduction of leaf water content to avoid desiccation and leaf drop (Gucci, Lombardini and Tattini, 1997). The enhanced ability of FR to exclude sodium from the roots and to maintain an elevated K^+/Na^+ ratio > 1 in control and 100 mM NaCl (Fig. 4, Table S4) supports the suggestion of a selective proton pump that is more effective for potassium ion influx in FR than in other cultivars under moderate salt stress conditions (Tattini, Melgar and Traversi, 2008). Conversely, the initial dramatic drop in root K^+ in FR roots with 200 mM NaCl represents a potential strategy among tolerant cultivars to limit sodium in root and shoot tissues (Hryvusevich et al., 2021; Pandolfi et al., 2017; Zhu, 2003).

The conclusion that osmotic stress coping mechanisms may mitigate the negative effects of salinity on photosynthetic parameters is supported by various observations made in the present study. First, the increased capacity to exclude sodium from the leaves in FR coincided with a better A_n rate than in the other cultivars (Tattini, Lombardini and Gucci, 1997). Likewise, a possible correlation could be made between the intercellular CO_2 concentration (C_i) and photosynthetic rates of all cultivars: cultivars with early reductions in photosynthetic rates, like LA, LE, and OL, had increased C_i values after 8 weeks. In contrast, the decrease in C_i and high photosynthetic rates in FR indicate better absorption and translocation of water and nutrients to the shoots (Table S4). The dramatic drop in A_n after salinity stress preserves a small quantity of water inside cells and prevents dehydration and degradation of the tissues (Ben Ahmed et al., 2008). This coincides with greater reductions in stomatal conductance rates in FR relative to the other three cultivars. This suggests that the reduced A_n rates in FR were more likely due to stomata-regulated supply limitations of CO_2 as C_i continued to be

assimilated at lower rates. In contrast, increased C_i in salt-treated LA, LE, and OL may have resulted from a decline in biochemical assimilation despite more stable stomatal conductance rates.

Furthermore, salinity treatments significatively affected the fluorescence parameters in all cultivars. In contrast to the data reported in previous studies (Bongi and Loreto, 1989; Kchaou et al., 2013), salinity treatments did not affect the maximum quantum yields of PSII (Fig. 2), suggesting that the increase of NPQ after eight weeks of salinity treatments is likely due to the activation of a protective mechanism for dissipating excess energy not used in photochemical reactions as has also been found in the case of *Oryza sativa* experiencing salinity stress (Nguyen et al., 2023) and *Zea mays* subjected to drought stress (Bashir et al., 2021). However, no significant increase of NPQ was observed in FR plants subjected to 100 mM NaCl treatment or in the early phase of the stress, indicating a greater capacity of this cultivar to continue performing photochemistry.

Olive trees may possess numerous mechanisms to prevent osmotic stress, including the sequestration of excess ions inside the vacuole. However, sequestration inside the vacuole increases the osmotic imbalance between it and the cytoplasm. For this reason, plants synthesize organic osmolytes such as sugars and polyphenols to assist their osmoregulation systems (Jogawat, 2019) in mitigating salinity stress with increased concentrations to reduce the oxidative damage caused by ROS (Sharma et al., 2019). In the present study, we verified that salinity stress stimulated the phenylpropanoid pathway in olive cultivars differently. Following salinity treatment, oleuropein was the most abundant polyphenol inside the leaves of all cultivars, particularly in FR. The increase of oleuropein reportedly helps to mitigate oxidative damage in olive leaves and substitute sugar to restore osmotic homeostasis inside root cells (Chartzoulakis et al., 2006). In contrast to Mechri and coworkers, an inverse relationship between oleuropein and verbascoside was not found in olive leaves in the present study (Mechri et al., 2019). Verbascoside may represent a specific polyphenol involved in avoiding osmotic stress for some cultivars. Increased production of quercetin, luteolin, and rutin has been correlated with limited water in roots and leaves (Ismail et al., 2016). Here, the enhancement of quercetin and rutin inside LA and FR leaves positively affected the K^+/Na^+ ratio when plants were grown in 100 and 200 mM NaCl, respectively (Table S4). These polyphenols can activate the SOS1 Na^+/H^+ transporter, likely leading FR and LA toward a better retention of K^+ and favoring sodium efflux into leaf mesophyll cells (Ismail et al., 2016; Parvin et al., 2019). The increased concentrations of luteolin in FR and LA may also be important for enhancing water uptake, stimulating α-amylase to increase soluble sugar concentrations in the leaves, reducing the expression of superoxide dismutase and catalase enzymes, and decreasing the levels of free radicals responsible for oxidative stress under salinity stress conditions (El-Shafey and AbdElgawad, 2014).

In this study, a complete analysis of the olive leaf proteome response to salinity stress demonstrates that the regulation of protein levels in olive leaf after salinity stress was largely genotype-dependent. Compared with FR and LE, OL and LA showed relatively restricted protein variations; the latter cultivars are generally selected for SHD systems due to their limited vigor and adaptability. Quantitative protein differences observed in FR and LE were more evident and representative for a discrimination between salinity-tolerant and -sensitive genotypes; thus, observed metabolic variations might be strictly linked to the ability of each cultivar to counteract salinity stress.

Some DPRs proteins deserve a specific discussion based on their nature and/or their previous recognition as abiotic/biotic stress response effectors. In particular, ferritin (AT5G01600.1, OE6A008047P3, OE6A113738P1) accumulated in FR and LE following exposure to a high salt concentration. By sequestering ions, this protein has been reported to protect plants from increased ROS levels deriving from the reaction between ferrous iron and H_2O_2 after various salinity and biotic stresses (Richards et al., 2015). This defense effect in FR and LE was also supported by the overrepresentation of chloroplastic ferredoxin-$NADP^+$-oxidoreductase (AT1G20020.1), which acts both as a protector against oxidative damage through the preservation of a high NADH/NADP ratio, and as mediator of the electron transfer between ferrodoxin and NADP during photosynthesis. The overrepresentation of this enzyme was observed in a biochemical study on olive plants undergoing salinity stress (Valderrama et al., 2007). Thylakoid lumen protein TLP18.3 (AT1G54780.1) was overrepresented in FR and OL and downrepresented in LE. This protein is known to be involved in regulating both degradation/synthesis of the oxidatively damaged D1 protein of PSII in the process of PSII repair (Järvi et al., 2016). Above-reported proteomic observations suggest that FR, unlike the other genotypes, implemented strategies to preserve its leaves from the oxidative insult deriving from salinity stress.

A similar consideration extended to both FR and LE can be proposed for two downrepresented proteins involved in response to external stimuli. In fact, dehydrin DHN1-like protein has already been reported as being deregulated under salinity stress conditions (Duan et al., 2022), and that dehydrins in general play an as playing an important role in drought stress by acting as a chaperone-like stabilizers shielding DNA from ROS-induced damage (Boddington and Graether, 2019) and by interacting with aquaporin proteins to regulate membrane permeability to water (Hernández-Sánchez et al., 2019). Similarly, BURP domain-containing RD22-like (AT5G25610.1) protein was widely reported being involved in the response to salinity stress (Harshavardhan et al., 2014; Sun et al., 2019), mitigating the osmotic imbalance in soybean and thale cress by regulating the increase of the lignin content of plant cells (Wang et al., 2012).

The most represented functional class of DRPs identified in olive cultivars in response to salinity stress was that of proteins involved in photosynthesis. Some isoforms of Lhcb3 (AT5G54270.1, 1365999475 and 1279004059) and of Lhcb5 (AT4G10340, OE6A066649P3, 1208530141 and OEU051766.2) were overrepresented in FR, LA and OL, while some were downrepresented in LE. These trimeric proteins belong to the light-harvesting complex II (LHCII) and are involved in protection against the damaging effects of excess energy under salt stress conditions, facilitating the energy dissipation by NPQ (Shu et al., 2019). Their overrepresentation in FR, LA and OL may contribute to improve energy dissipation and prevent the formation of ROS in leaves; conversely, downrepresentation of some Lhcbs in LE might determine a specific plant sensitivity to salinity stress due to its increased difficulty to dissipate excess photochemical energy. The latter condition might be balanced in LE through accumulating ubiquinol-cytochrome c oxidoreductase isoforms (AT3G52739.1, 1279051925 and 1278994309), which were also observed in FR. In fact, this enzyme promotes photosynthetic electron transport inside the chloroplast (Berry et al., 1991), thus counteracting excessive photochemical energy. On the other hand, CP12 (AT3G62410.1) was observed as selectively downrepresented in FR and LE. Since this protein is strictly known to be related to the photosynthetic rate and as a decremented descriptor of salinity stress in *Medicago sativa* (Xiong et al., 2017), we propose the same role here for specific olive cultivars subjected to saline irrigation. On the whole, information on deregulated photosynthetic proteins demonstrated that olive tree cultivars tend to preserve the efficiency of their photosynthetic activity in response to salinity stress through either the protection of the photosystems from ROS and the dissipation of detrimental photochemical energetic excesses.

Osmotic stress compensation inside the cell can be regulated by an increased representation of calmodulin-dependent protein phosphatase (AT3G43810.1), which forms calcineurin with Ca^{2+}. This protein was overrepresented and downrepresented in FR and LE, respectively. Calcineurin, together with increased Ca^{2+} inside the cell, is an intermediate of the signal transduction pathway related to salinity stress, which affects NaCl tolerance by regulating Na^+ influx and efflux (Yuenyong et al., 2018), and ion compartmentation into the vacuole (Manishankar et al., 2018). Overrepresentation of this protein in FR may explain the increased capacity of the corresponding leaves to exclude Na^+, while its

downrepresentation in LE might account for the observed sodium accumulation therein. In agreement with the Na^+ accumulation in LE was the specific, observed downrepresentation of ATEM6 (AT2G40170.1). This late embryogenesis abundant (LEA) protein has been associated with calcium protein kinase genes and with cell capacity to retain calcium to compensate for altered osmotic phenomena (Tang and Page, 2013). As with previous observations in *Oryza sativa, Gossipium hirsutum*, and *Pinus strobus* (Tang and Page, 2013), selective downrepresentation of ATEM6 in LE after NaCl stress can justify its putative role as a marker of salinity-sensitivity. Finally, the significant overrepresentation of Ser-Thr specific protein phosphatase (PP2A) (AT3G58500.1) in stressed FR confirmed the role of this protein in mitigating salinity stress through the regulation of cell metabolism and ion channels (Máthé et al., 2019; Chawla, Marothia and Pati, 2020).

5. Conclusion

This study provides a description of the adaptive processes ongoing in olive cultivars to confront salinity stress. Integrating physiological observations with different high throughput *omic* technologies allowed us to highlight a highly variable adaptative response in various cultivars in response to saline irrigation and to identify specific molecules linked to it. This resulted in a complete picture of cultivar-dependent mechanisms in response to salinity stress, and the possible identification of novel biomarkers for cultivar selection. Sodium exclusion, higher photosynthetic productivity and tissue water content were linked to increased production of selected polyphenols at moderate and high salt concentrations. This phenomenon was suggested as having a possible role in the measured improvement of K^+/Na^+ ratios, mitigation of oxidative stress and increased water absorption, respectively. Proteomic analysis highlighted an overrepresentation of proteins involved in regulating cellular metabolism, ion transport and dissipation of excess photochemical energy to mitigate salt stress in salt-tolerant cultivars. Increased sensitivity to salinity was linked to the downrepresentation of proteins involved in Ca^{2+} signaling and modulating redox reactions. Overall, the reported data underscore the complexity of olive tree responses salt stress.

Funding

This study was supported with funds from: i) Fondazione Caripit, Grant/Award Number: 2018.0527 to FV; ii) PON Ricerca ed Innovazione 2014-2020, azione II, PON ARS01_01136 for the project "E-Crops – Tecnologie per un'Agricoltura Digitale e Sostenibile" to AS; iii) Agritech National Research Center funded within the European Union NextGenerationEU program for the National Recovery and Resilience Plan, mission 4, component 2, investment 1.4 – D.D. 1032 published on 17/06/2022, project CN00000022 to AS. This manuscript reflects only the authors' views and opinions; neither the European Union nor European Commission can be considered responsible for them.

CRediT authorship contribution statement

Anna Maria Salzano: Formal analysis, Investigation, Marzia Vergine Formal analysis, Investigation, Writing – original draft, Writing – review & editing. **Carmine Negro**: Formal analysis, Investigation, Writing – original draft, Writing – review & editing. **Werther Guidi Nissim**: Conceptualization, Formal analysis, Investigation. **Raffaella Balestrini**: Writing – original draft, Writing – review & editing. **Maria Concetta de Pinto**: Writing – original draft, Writing – review & editing. **Stefania Fortunato**: Writing – original draft. **Gholamreza Gohari**: Writing – original draft, Writing – review & editing. **Stefano Mancuso**: Funding acquisition, Resources **Andrea Luvisi**: Writing – original draft, Writing – review & editing. **Luigi De Bellis**: Funding acquisition, Resources. **Andrea Scaloni**: Formal analysis, Funding acquisition, Investigation, Resources, Writing – original draft, Writing – review & editing. **Federico Vita**: Conceptualization, Data curation, Formal analysis, Funding acquisition, Investigation, Methodology, Resources, Software, Supervision, Validation, Writing – original draft.

Declaration of Competing Interest

The authors declare that they have no known competing financial interests or personal relationships that could have appeared to influence the work reported in this paper.

Data Availability

The data that supports the findings of this study are available in the Supporting Information.

Appendix A. Supporting information

Supplementary data associated with this article can be found in the online version at doi:10.1016/j.envexpbot.2023.105586.

References

Ahmed, C.Ben, Rouina, B.Ben, Boukhris, M., 2008. Changes in water relations, photosynthetic activity and proline accumulation in one-year-old olive trees (Olea europaea L. cv. Chemlali) in response to NaCl salinity. Acta Physiol. Plant. 30 (4), 553–560. https://doi.org/10.1007/s11738-008-0154-6.

Bashir, N., Athar, H.-U.-R., Kalaji, H.M., Wróbel, J., Mahmood, S., Zafar, Z.U., Ashraf, M., 2021. Is Photoprotection of PSII one of the key mechanisms for drought tolerance in maize. Int. J. Mol. Sci. 22, 13490. https://doi.org/10.3390/ijms222413490.

Ben Abdallah, M., et al., 2018. Unraveling physiological, biochemical and molecular mechanisms involved in olive (Olea europaea L. cv. Chétoui) tolerance to drought and salt stresses. J. Plant Physiol. 220, 83–95. https://doi.org/10.1016/j.jplph.2017.10.009.

Berry, E.A., Huang, L.S., DeRose, V.J., 1991. Ubiquinol-cytochrome c oxidoreductase of higher plants: Isolation and characterization of the bc1 complex from potato tuber mitochondria'. J. Biol. Chem. 266 (14), 9064–9077. https://doi.org/10.1016/s0021-9258(18)31553-9.

Besnard, G., Terral, J.F., Cornille, A., 2018. Erratum: on the origins and domestication of the olive: a review and perspectives (Annals of Botany DOI: 10.1093/aob/mcx145). Ann. Bot. 121 (3), 587–588. ⟨https://doi.org/10.1093/AOB/MCY002⟩.

Boddington, K.F., Graether, S.P., 2019. Binding of a *Vitis riparia* dehydrin to DNA. Plant Sci. 287, 110172 https://doi.org/10.1016/j.plantsci.2019.110172.

Bongi, G., Loreto, F., 1989. Gas-exchange properties of salt-stressed olive (Olea europea L.) leaves. Plant Physiol. 90 (4), 1408–1416. https://doi.org/10.1104/pp.90.4.1408.

Carillo, P. et al. (2011) 'Salinity Stress and Salt Tolerance', Abiotic Stress in Plants - Mechanisms and Adaptations [Preprint], (2014). https://doi.org/10.5772/22331.

Chartzoulakis, K., et al., 2002. Effects of NaCl salinity on growth, ion content and CO_2 assimilation rate of six olive cultivars. Sci. Hortic. 96 (1–4), 235–247. https://doi.org/10.1016/S0304-4238(02)00067-5.

Chartzoulakis, K., et al., 2006. Response of two olive cultivars to salt stress and potassium supplement. J. Plant Nutr. 29 (11), 2063–2078. https://doi.org/10.1080/01904160600932682.

Chawla, S., Marothia, D., Pati, P.K., 2020. Role of serine/threonine phosphatase PP2A class and its regulators in salinity stress tolerance in plants. Protein Phosphatases and Stress Management in Plants. Springer,, pp. 53–66. ⟨https://doi.org/10.1007/978-3-030-48733-1_4⟩.

Cimato, A., et al., 2010. An ecophysiological analysis of salinity tolerance in olive. Environ. Exp. Bot. 68 (2), 214–221. https://doi.org/10.1016/j.envexpbot.2009.12.006.

Daliakopoulos, I.N., et al., 2016. The threat of soil salinity: a European scale review. Sci. Total Environ. 573, 727–739. https://doi.org/10.1016/j.scitotenv.2016.08.177.

Duan, X., et al., 2022. Overexpression of a thioredoxin-protein-encoding gene, MsTRX, from medicago sativa enhances salt tolerance to transgenic tobacco. Agronomy 12 (6), 1467. https://doi.org/10.3390/agronomy12061467.

El Otmani, S., et al., 2021. Effects of olive cake and cactus cladodes as alternative feed resources on goat milk production and quality. Agric. (Switz.) 11 (1), 1–16. https://doi.org/10.3390/agriculture11010003.

El-Shafey, N.M., AbdElgawad, H., 2014. Luteolin, a bioactive flavone compound extracted from Cichorium endivia L. subsp. divaricatum alleviates the harmful effect of salinity on maize. Acta Physiol. Plant. 36 (6), 2165–2177. https://doi.org/10.1007/s11738-012-1017-8.

Fu, S., et al., 2010. Qualitative screening of phenolic compounds in olive leaf extracts by hyphenated liquid chromatography and preliminary evaluation of cytotoxic activity against human breast cancer cells. Anal. Bioanal. Chem. 397 (2), 643–654. https://doi.org/10.1007/s00216-010-3604-0.

Gucci, R., Tattini, M., 2010. Salinity tolerance in olive. Hortic. Rev. 21, 177–214. https://doi.org/10.1002/9780470650660.ch6.

Gucci, R., Lombardini, L., Tattini, M., 1997. Analysis of leaf water relations in leaves of two olive (Olea europaea) cultivars differing in tolerance to salinity. Tree Physiol. 17 (1), 13–21. https://doi.org/10.1093/treephys/17.1.13.

Guidi Nissim, W., et al., 2021. Willow and poplar for the phyto-treatment of landfill leachate in Mediterranean climate. J. Environ. Manag. 277, 111454 https://doi.org/10.1016/j.jenvman.2020.111454.

Harshavardhan, V.T., et al., 2014. AtRD22 and AtUSPL1, members of the plant-specific BURP domain family involved in Arabidopsis thaliana drought tolerance. PloS One 9 (10), e110065. https://doi.org/10.1371/journal.pone.0110065.

Hernández-Sánchez, I.E., Maruri-López, I., Molphe-Balch, E.P., Becerra-Flora, A., Jaimes-Miranda, F., Jiménez-Bremont, J.F., 2019. Evidence for in vivo interactions between dehydrins and the aquaporin *AtPIP2B*. Biochem. Biophys. Res. Commun. 510 (4), 545–550.

Hoagland, D.R.; Arnon, D.I. (1938) 'Agricultural Experiment Station the Water-Culture Method for Growing Plants Without Soil', California Experiment Station, C347(2nd edit), pp. 1–39.

Hryvusevich, P., Navaselsky, I., Talkachova, Y., Straltsova, D., Keisham, M., Viatoshkin, A., Samokhina, V., Smolich, I., Sokolik, A., Huang, X., Yu, M., Bhatla, S. C., Demidchik, V., 2021. Sodium influx and potassium efflux currents in sunflower root cells under high salinity. Front. Plant Sci. 11, 613936 https://doi.org/10.3389/fpls.2020.613936.

Ismail, H., et al., 2016. Rutin, a flavonoid with antioxidant activity, improves plant salinity tolerance by regulating K+ retention and Na+ exclusion from leaf mesophyll in quinoa and broad beans. Funct. Plant Biol. 43 (1), 75–86. https://doi.org/10.1071/FP15312.

Järvi, S., Isojärvi, J., Kangasjärvi, S., Salojärvi, J., Mamedov, F., Suorsa, M., Aro, E.M., 2016. Photosystem II repair and plant immunity: lessons learned from Arabidopsis mutant lacking the thylakoid lumen protein 18.3. Front. Plant Sci. 7, 148–160.

Jogawat, A., 2019. Osmolytes and their Role in Abiotic Stress Tolerance in Plants. Mol. Plant Abiotic Stress.: Biol. Biotechnol. 91–104. https://doi.org/10.1002/9781119463665.ch5.

Kchaou, H., et al., 2013. Genotypic differentiation in the stomatal response to salinity and contrasting photosynthetic and photoprotection responses in five olive (Olea europaea L.) cultivars. Sci. Hortic. 160, 129–138. https://doi.org/10.1016/j.scienta.2013.05.030.

Llanes, A., Palchetti, M.V., Vilo, C., Ibañez, C., 2021. Molecular control to salt tolerance mechanisms of woody plants: recent achievements and perspectives. Ann. For. Sci. 78, 96 https://doi.org/10.1007/s13595-021-01107-7.

Loupassaki, M.H., et al., 2002. Effects of salt stress on concentration of nitrogen, phosphorus, potassium, calcium, magnesium, and sodium in leaves, shoots, and roots of six olive cultivars. J. Plant Nutr. 25 (11), 2457–2482. https://doi.org/10.1081/PLN-120014707.

Lozano-Sánchez, J., et al., 2010. Prediction of extra virgin olive oil varieties through their phenolic profile. potential cytotoxic activity against human breast cancer cells. J. Agric. Food Chem. 58 (18), 9942–9955. https://doi.org/10.1021/jf101502q.

Maas, E.V., Grattan, S.R., 2015. Crop yields as affected by salinity. Agric. Drain. 38, 55–108. https://doi.org/10.1002/9780891182306.ch03.

Manishankar, P., Wang, N., Köster, P., Alatar, A.A., Kudla, J., 2018. Calcium signaling during salt stress and in the regulation of ion homeostasis. J. Exp. Bot. 69 (17), 4215–4226. https://doi.org/10.1093/jxb/ery201.

Máthé, C., et al., 2019. The role of serine-threonine protein phosphatase pp2a in plant oxidative stress signaling—facts and hypotheses. Int. J. Mol. Sci. 20 (12), 3028. https://doi.org/10.3390/ijms20123028.

Mechri, B., et al., 2019. Root verbascoside and oleuropein are potential indicators of drought resistance in olive trees (Olea europaea L.). Plant Physiol. Biochem. 141, 407–414. https://doi.org/10.1016/j.plaphy.2019.06.024.

Mousavi, S., et al., 2019. Plasticity of fruit and oil traits in olive among different environments. Sci. Rep. 9 (1), 1–13. https://doi.org/10.1038/s41598-019-53169-3.

Mousavi, S., et al., 2022. Characterization of Differentially Expressed Genes under Salt Stress in Olive, 2022 Int. J. Mol. Sci. 23 (1), 154. https://doi.org/10.3390/ijms23010154.

Munns, R., Tester, M., 2008. Mechanisms of salinity tolerance. Annu Rev Plant Biol. 59, 651–681.

Nguyen, A.T., Tran, L.H., Jung, S., 2023. Salt Stress-Induced Modulation of Porphyrin Biosynthesis, Photoprotection, and Antioxidant Properties in Rice Plants (*Oryza sativa*). Antioxidants 12, 1618. https://doi.org/10.3390/antiox12081618.

Pandolfi, C., et al., 2017. Salt acclimation process: A comparison between a sensitive and a tolerant Olea europaea cultivar. Tree Physiol. 37 (3), 380–388. https://doi.org/10.1093/treephys/tpw127.

Parvin, K., et al., 2019. Quercetin mediated salt tolerance in tomato through the enhancement of plant antioxidant defense and glyoxalase systems. Plants 8 (8), 247. https://doi.org/10.3390/plants8080247.

Quirantes-Piné, R., et al., 2013. A metabolite-profiling approach to assess the uptake and metabolism of phenolic compounds from olive leaves in SKBR3 cells by HPLC-ESI-QTOF-MS. J. Pharm. Biomed. Anal. 72, 121–126. https://doi.org/10.1016/j.jpba.2012.09.029.

Richards, S.L., et al., 2015. The hydroxyl radical in plants: From seed to seed. J. Exp. Bot. 66 (1), 37–46. https://doi.org/10.1093/jxb/eru398.

Salzano, A.M., et al., 2019. Unveiling kiwifruit metabolite and protein changes in the course of postharvest cold storage. Front. Plant Sci. 10, 71 https://doi.org/10.3389/fpls.2019.00071.

Sharma, A., et al., 2019. Response of phenylpropanoid pathway and the role of polyphenols in plants under abiotic stress. Molecules 24 (13), 2452. https://doi.org/10.3390/molecules24132452.

Shu, S., et al., 2019. The positive regulation of putrescine on light-harvesting complex II and excitation energy dissipation in salt-stressed cucumber seedlings. Environ. Exp. Bot. 162, 283–294. https://doi.org/10.1016/j.envexpbot.2019.02.027.

Skodra, C., Michailidis, M., Moysiadis, T., Stamatakis, G., Ganopoulou, M., Adamakis, I. D.S., Angelis, L., Ganopoulos, I., Tanou, G., Samiotaki, M., Bazakos, C., Molassiotis, A., 2023. Disclosing the molecular basis of salinity priming in olive trees using proteogenomic model discovery. Plant Physiol. 191 (3), 1913–1933. https://doi.org/10.1093/plphys/kiac572.

Sun, H., Wei, H., Wang, H., Hao, P., Gu, L., Liu, G., Ma, L., Su, Z., Yu, S., 2019. Genome-wide identification and expression analysis of the BURP domain-containing genes in *Gossypium hirsutum*. BMC Genom. 20 (1), 558.

Taamalli, A., et al., 2012. Use of advanced techniques for the extraction of phenolic compounds from Tunisian olive leaves: Phenolic composition and cytotoxicity against human breast cancer cells. Food Chem. Toxicol. 50 (6), 1817–1825. https://doi.org/10.1016/j.fct.2012.02.090.

Taamalli, A., et al., 2013. Characterisation of phenolic compounds by HPLC-TOF/IT/MS in buds and open flowers of "chemlali" olive cultivar. Phytochem. Anal. 24 (5), 504–512. https://doi.org/10.1002/pca.2450.

Talhaoui, N., et al., 2014. Determination of phenolic compounds of "Sikitita" olive leaves by HPLC-DAD-TOF-MS. Comparison with its parents "Arbequina" and "Picual" olive leaves. ', Lwt 58 (1), 28–34. https://doi.org/10.1016/j.lwt.2014.03.014.

Talhaoui, N., et al., 2015. Chemometric analysis for the evaluation of phenolic patterns in olive leaves from six cultivars at different growth stages. J. Agric. Food Chem. 63 (6), 1722–1729. https://doi.org/10.1021/jf5058205.

Tang, W., Page, M., 2013. Overexpression of the Arabidopsis AtEm6 gene enhances salt tolerance in transgenic rice cell lines. Plant Cell, Tissue Organ Cult. 114 (3), 339–350. https://doi.org/10.1007/s11240-013-0329-8.

Tattini, M., Lombardini, L., Gucci, R., 1997. 'The effect of NaCl stress and relief on gas exchange properties of two olive cultivars differing in tolerance to salinity'. Plant Soil 197 (1), 87–93. https://doi.org/10.1023/A:1004241628878.

Tóth, G. et al. (2008) 'Update map of salt affected soils in the European Union', Threats to soil quality in Europe, (January 2014), pp. 67–77.

Tous, J., 2011. Olive production systems and mechanization. Acta Hortic. 169–184. https://doi.org/10.17660/ActaHortic.2011.924.22.

Valderrama, R., et al., 2007. Nitrosative stress in plants. FEBS Lett. 581 (3), 453–461. https://doi.org/10.1016/j.febslet.2007.01.006.

Vergine, M., et al., 2022. Phenolic characterization of olive genotypes potentially resistant to Xylella. J. Plant Interact. 17 (1), 462–474. https://doi.org/10.1080/17429145.2022.2049381.

Wang, H., et al., 2012. Expression of an apoplast-localized BURP-domain protein from soybean (GmRD22) enhances tolerance towards abiotic stress. Plant, Cell Environ. 35 (11), 1932–1947. https://doi.org/10.1111/j.1365-3040.2012.02526.x.

Wiśniewski, J.R., et al., 2009. Universal sample preparation method for proteome analysis. Nat. Methods 6 (5), 359–362. https://doi.org/10.1038/nmeth.1322.

Xiong, J., et al., 2017. Proteomic analysis of early salt stress responsive proteins in alfalfa roots and shoots. Proteome Sci. 15 (1), 1–19. https://doi.org/10.1186/s12953-017-0127-z.

Yuenyong, W., et al., 2018. Downstream components of the calmodulin signaling pathway in the rice salt stress response revealed by transcriptome profiling and target identification. BMC Plant Biol. 18 (1), 335 https://doi.org/10.1186/s12870-018-1538-4.

Zhu, J.K., 2003. Regulation of ion homeostasis under salt stress. Curr. Opin. Plant Biol. 6 (5), 441–445. https://doi.org/10.1016/S1369-5266(03)00085-2.